SIAM J. APPL. MATH.
Vol. 76, No. 3, pp. 1191–1218

TWISTED X-RAYS: INCOMING WAVEFORMS YIELDING DISCRETE DIFFRACTION PATTERNS FOR HELICAL STRUCTURES*

GERO FRIESECKE†, RICHARD D. JAMES‡, AND DOMINIK JÜSTEL†

Abstract. Conventional X-ray methods use incoming plane waves which result in discrete diffraction patterns when scattered at crystals. Here we find, by a systematic method, incoming waveforms which exhibit discrete diffraction patterns when scattered at helical structures. As examples we present simulated diffraction patterns of carbon nanotubes and tobacco mosaic virus. The new incoming waveforms, which we call *twisted waves* due to their geometric shape, are found theoretically as closed-form solutions to Maxwell's equations. The theory of the ensuing diffraction patterns is developed in detail. A twisted analogue of the Von Laue condition is seen to hold, with the peak locations encoding the symmetry and the helix parameters, and the peak intensities indicating the electronic structure in the unit cell. If suitable twisted X-ray sources can in the future be realized experimentally, it appears from our mathematical results that they will provide a powerful tool for directly determining the detailed atomic structure of numerous biomolecules and nanostructures with helical symmetries. This would eliminate the need to crystallize those structures or their subunits.

Key words. X-ray diffraction, helical structure, crystallography, Maxwell equations, Poisson summation

AMS subject classifications. 78A45, 35Q61, 43A25

DOI. 10.1137/15M1043418

1. Introduction.

This paper explores—at the level of modeling and simulation—the possibility of novel X-ray methods for the determination of the detailed atomic structure of highly regular but not periodic molecules. The details are worked out for helical structures. These include carbon nanotubes, the necks and tails of viruses, and many of the common proteins (actin, collagen). The quest for novel methods is motivated by the fact that current X-ray methods, while hugely successful, have important shortcomings. A native helical assembly of proteins either has to be broken at the outset and the proteins crystallized, which is difficult and may lead to non-native forms; or one uses X-ray fiber diffraction, which resolves only the axial but not the angular symmetry into sharp peaks.

Roughly, our idea is the following. Conventional X-ray methods use incoming plane waves

$$\mathbf{E}(\mathbf{x},t) = \mathbf{n}e^{i(\mathbf{k}\cdot\mathbf{x}-\omega t)}, \quad \mathbf{B}(\mathbf{x},t) = \tfrac{1}{\omega}(\mathbf{k}\times\mathbf{n})e^{i(\mathbf{k}\cdot\mathbf{x}-\omega t)}, \tag{1.1}$$

and result (in the relevant regime of X-ray wavelength $\ll$ sample diameter $\ll$ distance

*Received by the editors October 12, 2015; accepted for publication (in revised form) April 14, 2016; published electronically June 23, 2016.
http://www.siam.org/journals/siap/76-3/M104341.html

†Faculty of Mathematics, Technical University of Munich, 85748, Garching, Germany (gf@ma.tum.de, juestel@ma.tum.de). The first author's research was partially supported by the DFG through SFB-TR 109. The third author's research was partially supported by a stipend from Universität Bayern e.V.

‡Department of Aerospace Engineering and Mechanics, University of Minnesota, Minneapolis, MN 55455 (james@umn.edu). This author's research was supported by the AFOSR (FA9550-15-1-0207) and partially supported by the ONR (N00014-14-0714), an NSF/PIRE grant (OISE-0967140), the MURI program (FA9550-12-1-0458), and a John Von Neumann visiting professorship at Technical University of Munich.

of detector from sample, Fresnel number $\ll 1$) in the outgoing field

$$\mathbf{E}_{out}(\mathbf{x},t) = -\frac{\text{const}}{|\mathbf{x}-\mathbf{x}_c|}\,\mathbf{n}' e^{i(\mathbf{k}'(\mathbf{x})\cdot\mathbf{x}-\omega t)} \int_\Omega e^{-i(\mathbf{k}'(\mathbf{x})-\mathbf{k})\cdot\mathbf{y}}\rho(\mathbf{y})\,d\mathbf{y}, \tag{1.2}$$

with polarization vector $\mathbf{n}' = (\mathbf{I} - \frac{\mathbf{k}'}{|\mathbf{k}'|}\otimes\frac{\mathbf{k}'}{|\mathbf{k}'|})\mathbf{n}$ and outgoing wavevector $\mathbf{k}'(\mathbf{x}) = |\mathbf{k}|\frac{\mathbf{x}-\mathbf{x}_c}{|\mathbf{x}-\mathbf{x}_c|}$. Here ρ is the electron density of the illuminated sample, Ω is a finite three-dimensional region occupied by the sample, $\mathbf{x}_c$ denotes a typical point in the sample, $\mathbf{I}$ is the 3×3 identity matrix, $\mathbf{a}\otimes\mathbf{b}$ denotes the 3×3 matrix $\mathbf{a}\,\mathbf{b}^T$, and $|\mathbf{a}|$ is the euclidean norm of the vector $\mathbf{a}$.

The emergence of the Fourier transform in (1.2), and its amazing properties regarding constructive/destructive interference, underlie the power of X-ray methods for periodic structures. One can see from (1.2) and its derivation that the Fourier integral kernel $e^{-i(\mathbf{k}'-\mathbf{k})\cdot\mathbf{y}}$ is directly arising from the assumption of a plane-wave source (1.1). Other sources would give other kernels. This suggests the following line of research: *design the incoming radiation (as a solution of Maxwell's equations) such that the kernel interacts with highly symmetric but noncrystalline structures with the same dramatic properties of constructive/destructive interference as occurs in the periodic case.*

This design problem for the incoming waves can be formalized into the following mathematical problem: *find time-harmonic solutions to Maxwell's equations which are simultaneous eigenfunctions of a continuous extension of the generating symmetry group of the structure.* Why this is a good formalization is a long story, told in section 4.

For discrete translation groups, which are the generating symmetries of crystals, we show that the design problem is solved precisely by the plane waves used in classical X-ray methods. This is a new characterization of electromagnetic plane waves. It explains why plane waves are right for crystals.

For helical symmetry groups, the design problem can also be completely solved. The ensuing family of incoming waves is

$$\mathbf{E}(r,\varphi,z,t) = e^{i(\alpha\varphi+\beta z-\omega t)} \begin{pmatrix} \cos\varphi & -\sin\varphi & 0 \\ \sin\varphi & \cos\varphi & 0 \\ 0 & 0 & 1 \end{pmatrix} \begin{pmatrix} \frac{n_1+in_2}{2} & \frac{n_1-in_2}{2} & 0 \\ \frac{n_2-in_1}{2} & \frac{n_2+in_1}{2} & 0 \\ 0 & 0 & n_3 \end{pmatrix} \begin{pmatrix} J_{\alpha+1}(\gamma r) \\ J_{\alpha-1}(\gamma r) \\ J_\alpha(\gamma r) \end{pmatrix}, \tag{1.3}$$

where $(\alpha,\beta,\gamma)\in\mathbb{Z}\times\mathbb{R}\times(0,\infty)$ is a parameter vector analogous to the wavevector $\mathbf{k}$ in (1.1), $\mathbf{n}\in\mathbb{C}^3$ is a polarization vector which must satisfy $(0,\gamma,\beta)\cdot\mathbf{n}=0$, and the frequency ω is given by $\omega = c|(0,\gamma,\beta)|$. The cartesian vector $(0,\gamma,\beta)$ has a simple physical meaning which will emerge when decomposing twisted waves into plane waves (see (6.21)). The J_α are Bessel functions, (r,φ,z) are cylindrical coordinates with respect to the helical axis, and $\mathbf{E}$ is the cartesian field vector with respect to a fixed basis of $\mathbb{R}^3$, with the third component corresponding to the axial direction. We call the electric fields (1.3) *twisted waves.* Figure 1 shows the twisted wave with parameter vector $(\alpha,\beta,\gamma)=(5,3,1)$ and polarization vector $\mathbf{n}=(1,0,0)$.

Thus twisted waves consist of four factors: a scalar plane wave on the cylinder; a rotation matrix which rotates the field direction along with the base point; a somewhat mysterious polarization tensor which depends on the polarization vector; and a vector of three Bessel functions of neighboring order.

Twisted waves exhibit orbital angular momentum (OAM). In fact, they are eigenstates of the correctly defined [CT97] angular momentum operator on vector fields (see section 6). Intriguingly, similar waveforms have been experimentally realized, such

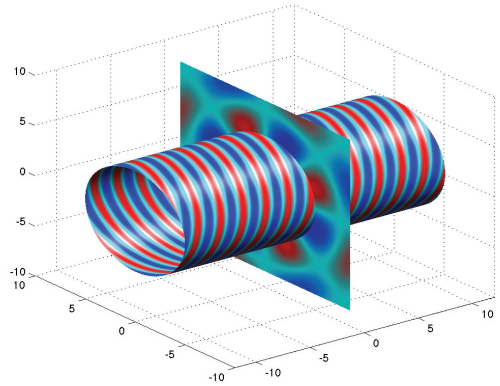

FIG. 1. *A twisted wave with angular, axial, and radial wavenumbers* $(\alpha, \beta, \gamma) = (5, 3, 1)$. *The plot shows the real part of the first component of the wave. Red: positive values; Blue: negative values. Note the helical shape of the level sets restricted to a co-axial cylinder, and the Bessel pattern perpendicular to the axis.*

as optical higher-order Bessel beams [AD00] and photons and beams carrying OAM [AB92, HD92, MTT07]. A related recent development is the creation of electron vortex beams [UT10, VTS10]. The detailed form (1.3) differs somewhat from previously reported OAM waveforms. Scalar Bessel beams as reported in [AD00] describe the individual twisted-wave components but not their interplay; and the Laguerre–Gauss vector beam reported in [AB92] is well-approximated in the focus region by a Hansen cylindrical vector harmonic [Ha34] with transversal pilot vector $\mathbf{a}$, but the latter is not quite a twisted wave either.[1]

The helical shape of the level sets in Figure 1 suggests that for suitable values of the angular and axial wavenumbers, twisted waves can induce resonant electronic oscillations of every single molecule in a structure with helical architecture. Thus one can hope for diffraction intensities which strongly depend on the twisted wave parameters.

At least in the axial direction, the radiation scattered by a helical structure indeed exhibits sharp discrete peaks with respect to the radiation parameters α and β. More precisely, *the signal of a helical structure in the axial direction vanishes unless the angular/axial wavenumbers of the twisted wave minus the axial wavenumber of the outgoing wave belong to the reciprocal helical lattice shifted left or right by precisely one angular wavenumber.* This is an analogue of the Von Laue condition, but waves and structure are curved. The shifts come from the fact that the polarization direction of a twisted wave rotates along with the base point. Details are given in section 8. Moreover, as in X-ray crystallography, the unit cell electron density can be recovered, up to a scalar phase problem, from the peak intensities. A further attractive feature is that the outgoing signal is invariant under axial translations and rotations of the structure.[2]

[1]The Hansen vector harmonics are defined as $\operatorname{curl}(\mathbf{a}\psi)$ and $\operatorname{curl}\operatorname{curl}(\mathbf{a}\psi)$, where ψ is a scalar cylindrical harmonic, i.e., $\psi(r, \varphi, z) = e^{i(\alpha\varphi+\beta z)} J_\alpha(\gamma r)$, and $\mathbf{a} \in \mathbb{R}^3$ is a fixed "pilot vector". One can check that the axial choice $\mathbf{a} = (0, 0, a_3)$ yields the waveform (1.3) with $\mathbf{n} = (ia_3\gamma, 0, 0)$ (respectively, $\mathbf{n} = a_3\gamma(0, -\beta, \gamma)$), but any other choice of $\mathbf{a}$ does not yield a twisted wave, and conversely any other twisted wave is not a Hansen vector harmonic.

[2]By comparison, the signal produced by fiber diffraction as described by the Cochran–Crick–Vand formula [CCV52] is not invariant under axial rotations, causing well-known difficulties in the interpretation of fiber diffraction images.

These results suggest a hypothetical set-up of structure analysis with twisted X-rays. Send a twisted wave towards a co-axial helical structure. Use a detector further along the axis to record the diffracted intensities as a function of the incoming radiation parameters. Solve a scalar phase problem to infer the electron density. See Figure 2.

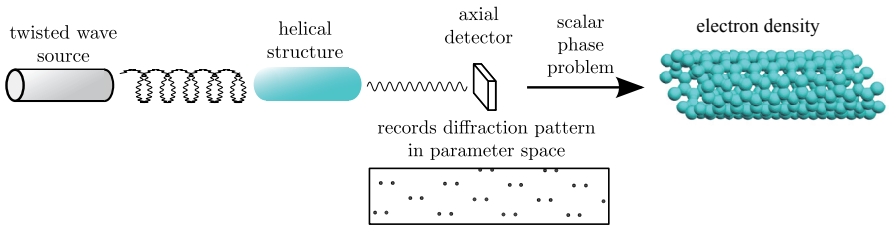

FIG. 2. *Hypothetical set-up of structure analysis with twisted X-rays.*

The plan of the paper is as follows. Section 2 extends the standard scalar Fourier transform model for plane-wave diffraction to a vector-valued electromagnetic model needed to treat general incoming waveforms. Sections 4–6 formulate the radiation design problem and derive plane waves and twisted waves from it. Sections 7–9 develop the theory of diffraction patterns of twisted X-rays. Finally, in section 10 we present simulated diffraction patterns of a carbon nanotube and of tobacco mosaic virus. Some of the results presented here were announced in [JFJ16].

2. Electromagnetic model for the diffracted radiation. Incoming electromagnetic waves will be sought as solutions to Maxwell's equations in vacuum,

$$\frac{1}{c^2}\frac{\partial \mathbf{E}}{\partial t} = \operatorname{curl} \mathbf{B}, \quad \operatorname{div} \mathbf{E} = 0, \quad \frac{\partial \mathbf{B}}{\partial t} = -\operatorname{curl} \mathbf{E}, \quad \operatorname{div} \mathbf{B} = 0, \tag{2.1}$$

which are time-harmonic, that is, $\mathbf{E}(\mathbf{x}, t) = \mathbf{E}_0(\mathbf{x})e^{-i\omega t}$, $\mathbf{B}(\mathbf{x}, t) = \mathbf{B}_0(\mathbf{x})e^{-i\omega t}$ for some $\omega > 0$. Here $\mathbf{E}$ and $\mathbf{B}$ are the electric and magnetic fields and c is the speed of light. SI units are used throughout. The fields are defined on $\mathbb{R}^3 \times [0, \infty)$ and take values in $\mathbb{C}^3$. This ansatz reduces Maxwell's equations (2.1) to

$$\Delta \mathbf{E}_0 = -\frac{\omega^2}{c^2}\mathbf{E}_0, \quad \operatorname{div} \mathbf{E}_0 = 0, \tag{2.2}$$

$$\mathbf{B}_0 = -\frac{i}{\omega}\operatorname{curl} \mathbf{E}_0. \tag{2.3}$$

We are interested in bounded solutions to (2.2)–(2.3). A basic example, and the one used in classical X-ray crystallography, are plane waves

$$\mathbf{E}_0(\mathbf{x}) = \mathbf{n}e^{i\mathbf{k}_0\cdot\mathbf{x}}, \quad \mathbf{B}_0(\mathbf{x}) = \frac{1}{\omega}(\mathbf{k}_0 \times \mathbf{n})e^{i\mathbf{k}_0\cdot\mathbf{x}}, \quad \text{where } |\mathbf{k}_0| = \frac{\omega}{c}, \quad \mathbf{k}_0 \cdot \mathbf{n} = 0. \tag{2.4}$$

Here $\mathbf{k}_0$ (the wavevector) and $\mathbf{n}$ (the polarization vector) are arbitrary vectors in $\mathbb{R}^3$ and $\mathbb{C}^3$ satisfying the two conditions in (2.4). Time frequency, wavevector, and wavelength λ are related by $\lambda = 2\pi/|\mathbf{k}_0| = 2\pi\frac{c}{\omega}$. The last expression provides a meaningful definition of wavelength for general time-harmonic solutions to Maxwell's equations.

The standard scalar Fourier transform model or *oscillator model* of X-ray diffraction patterns (see, e.g., [AM76]) which underlies the crystallography and biocrystallography literature is insufficient for our purposes. We are seeking incoming waves

which exhibit resonances with, say, helical structures, and—as it turns out—these will necessarily contain fluctuating polarization directions. As a consequence we need a full electromagnetic (vector-valued) extension of the standard model.

Such an electromagnetic model can be obtained as follows. Consider any electron density $\rho(\mathbf{y})$, $\mathbf{y} \in \mathbb{R}^3$, and a classical model of the electrons driven by the incoming fields and producing the well-known Lienard–Wiechert fields [Gr99]. Pass to a nonrelativistic (weak-field) limit; superpose fields from all the electrons; and make a far field approximation X-ray wavelength $\ll$ sample diameter $\ll$ distance between sample and detector, Fresnel number $\ll 1$. The details can be found in our companion paper [FJJ16]. The resulting expression for the diffracted electromagnetic field is

(2.5)
$$\mathbf{E}_{out}(\mathbf{x},t) = -\,c_{e\ell}\,\frac{e^{i(\mathbf{k}'(\mathbf{x})\cdot\mathbf{x}-\omega t)}}{|\mathbf{x}-\mathbf{x}_c|}\left(\mathbf{I}-\frac{\mathbf{k}'(\mathbf{x})}{|\mathbf{k}'(\mathbf{x})|}\otimes\frac{\mathbf{k}'(\mathbf{x})}{|\mathbf{k}'(\mathbf{x})|}\right)\int_{\mathbb{R}^3}\mathbf{E}_0(\mathbf{y})\rho(\mathbf{y})\,e^{-i\mathbf{k}'(\mathbf{x})\cdot\mathbf{y}}d\mathbf{y},$$
$$\mathbf{B}_{out}(\mathbf{x},t) = \frac{1}{\omega}\,\mathbf{k}'(\mathbf{x})\,\times\,\mathbf{E}_{out}(\mathbf{x},t),$$

with outgoing wavevector familiar from the oscillator model,

$$\mathbf{k}'(\mathbf{x}) = \frac{\omega}{c}\frac{\mathbf{x}-\mathbf{x}_c}{|\mathbf{x}-\mathbf{x}_c|}. \tag{2.6}$$

(The diffraction model (2.5)–(2.6) is standard, though only special cases or pieces are given in textbooks.) Here $\mathbf{E}_0(y)e^{-i\omega t}$ is the incoming electric field, a solution to the time-harmonic Maxwell equation (2.2), $\rho : \mathbb{R}^3 \to \mathbb{R}$ is the electron density of the sample, $\mathbf{x}_c$ is a typical point in the sample, and $c_{e\ell}$ is a universal constant depending, among other things, on the charge and mass of the electron.

If the incoming electromagnetic field is replaced by its real part, as it properly should to model physical incoming X-rays, the diffracted radiation is given by the real part of (2.5).

According to the model (2.5)–(2.6), the outgoing wavevectors $\mathbf{k}'$ have the same length as the incoming wavevector $\mathbf{k}$, i.e., $|\mathbf{k}'| = |\mathbf{k}|$. This relation has the important microscopic physical interpretation that the photon energy is conserved in the scattering. Note that the energy of a photon with wavevector $\mathbf{k}$ is $E = |\mathbf{p}|c$, where $\mathbf{p} = \hbar\mathbf{k}$ is the photon momentum. Thus the model (2.5)–(2.6) corresponds to *elastic* or *Thomson* scattering.

For incoming plane waves (2.4), equation (2.5) for the electromagnetic field reduces to

(2.7)
$$\mathbf{E}_{out}(\mathbf{x},t) = -\,c_{e\ell}\,\frac{e^{i(\mathbf{k}'(\mathbf{x})\cdot\mathbf{x}-\omega t)}}{|\mathbf{x}-\mathbf{x}_c|}\mathbf{n}'(\mathbf{x})\,f(\mathbf{k}'(\mathbf{x})-\mathbf{k}_0),\quad \mathbf{B}_{out}(\mathbf{x},t) = \frac{1}{\omega}\mathbf{k}'(\mathbf{x})\times\mathbf{E}_{out}(\mathbf{x},t),$$

with scalar integral factor and outgoing direction-dependent polarization vector

$$f(\mathbf{k}'-\mathbf{k}_0) = \int_{\mathbb{R}^3} e^{-i(\mathbf{k}'-\mathbf{k}_0)\cdot\mathbf{y}}\rho(\mathbf{y})\,d\mathbf{y},\quad \mathbf{n}'(\mathbf{x}) = \left(\mathbf{I}-\frac{\mathbf{k}'(\mathbf{x})}{|\mathbf{k}'(\mathbf{x})|}\otimes\frac{\mathbf{k}'(\mathbf{x})}{|\mathbf{k}'(\mathbf{x})|}\right)\mathbf{n}. \tag{2.8}$$

The integral factor f appearing in (2.8) is just the well-known *structure factor* or *form factor* or *scattering factor* [Gr99, Ja98, AM76, AM11]. Mathematically, it is the Fourier transform of the electron density, evaluated at the difference $\mathbf{k}'-\mathbf{k}$ of the outgoing and incoming wavevectors. The expressions (2.8) including that for $\mathbf{n}'$ agree with the result derived in [Sa09] from perturbative nonrelativistic quantum electrodynamics (QED).

In X-ray experiments the electromagnetic fields $\mathbf{E}$ and $\mathbf{B}$ cannot be measured directly; a detector only records the scalar field intensity. The latter is defined (see, e.g., [Gr99]) as the *time average of the absolute value of the Poynting vector* and has the physical dimension of power transferred per unit area, i.e., energy transferred per unit area per unit time. In formulae,

$$I(\mathbf{x}) = \lim_{T\to\infty} \frac{1}{T}\int_0^T |\mathbf{S}(\mathbf{x},t)|\,dt, \quad \mathbf{S}(\mathbf{x},t) = \frac{1}{\mu_0}\operatorname{Re}\mathbf{E}_{out}(\mathbf{x},t)\times \operatorname{Re}\mathbf{B}_{out}(\mathbf{x},t). \tag{2.9}$$

Here and below, μ_0 and ε_0 are the magnetic and electric constants, which are related to the speed of light by the equation $\varepsilon_0\mu_0 = 1/c^2$, and $\mathbf{S}$ denotes the Poynting vector. Note that the latter is the flux vector for the energy density $e = \frac{1}{2}(\varepsilon_0|\operatorname{Re}\mathbf{E}|^2 + |\operatorname{Re}\mathbf{B}|^2/\mu_0)$ in Maxwell's equation. It can be shown via standard arguments (see [FJJ16]) that the intensity of the outgoing field at the observation point $\mathbf{x}$ is in our case equal to

$$I(\mathbf{x}) = \frac{c\,\varepsilon_0}{2}\,|\mathbf{E}_{out}(\mathbf{x},t)|^2, \tag{2.10}$$

where $\mathbf{E}_{out}$ is the complex electric field in (2.5) (note that its absolute value is independent of t). The appearance of the *complex* field amplitude comes from the time averaging in (2.9).

In particular, by (2.7), (2.8), the data gathered from a sufficiently large set of observation points $\mathbf{x}$ and incoming plane-wave wavevectors $\mathbf{k}_0$ delivers the abstract data set

$$|\hat{\rho}(\mathbf{k})|^2, \quad \mathbf{k}\in\mathbb{R}^d, \tag{2.11}$$

and the X-ray interpretation problem, i.e., the task of inferring atomic structure, ρ, from X-ray diffraction data, $|\hat{\rho}|^2$, reduces to the phase problem for the Fourier transform. Note that the data set (2.11) is a function on the dual (wavevector) space of the physical space on which the density is defined. The abstract "diffraction intensity" or "diffraction spectrum" or "diffraction measure" (2.11) constitutes the starting point of previous mathematical work on X-ray diffraction of crystals [St94, Fr07] and quasicrystals [Ho95, BM04, BG08, BG13].

For general incoming radiation, it will be useful to interpret the integral in (2.5) physically as a generalized structure factor and mathematically as an integral transform that depends on the incoming field $\mathbf{E}_0$ and maps the electronic charge density ρ to a vector field on the dual (wavevector) space,

$$\mathbf{f}_{\mathbf{E}_0}(\mathbf{k}) = (\mathcal{R}_{\mathbf{E}_0}\rho)(\mathbf{k}) = \int_{\mathbb{R}^3} \mathbf{E}_0(\mathbf{y})\rho(\mathbf{y})e^{-i\mathbf{k}\cdot\mathbf{y}}d\mathbf{y} \quad (\mathbf{k}\in\mathbb{R}^3). \tag{2.12}$$

For plane waves, this expression is just the Fourier transform of ρ multiplied by the incoming polarization. Thus the expression (2.12) generalizes the Fourier transform, and might be called the *radiation transform* of ρ with respect to $\mathbf{E}_0$. For any bounded solution to the time-harmonic Maxwell equation (2.2), equation (2.12) naturally establishes $\mathcal{R}_{\mathbf{E}_0}$ as a linear map from $L^1(\mathbb{R}^3)$ to the space of bounded continuous vector fields on the dual (wavevector) space $\mathbb{R}^3$. Like the Fourier transform, it can be extended to tempered distributions and maps these to vector-valued tempered distributions. This extension will be useful when discussing diffraction in the idealized but important case of infinite helices, nanotubes, and crystals.

3. Classical Von Laue condition. Given a complete mathematical model of the outgoing electromagnetic field such as (2.5), we can cast the Von Laue condition of classical X-ray crystallography [FKL12] in the form of a mathematical theorem. Let $\mathcal{L}$ be a Bravais lattice in $\mathbb{R}^3$, i.e., a set of the form

$$\mathcal{L} = A\,\mathbb{Z}^3 \quad \text{for some invertible } 3\times 3 \text{ matrix } A. \tag{3.1}$$

Let ρ be any smooth $\mathcal{L}$-periodic function on $\mathbb{R}^3$. Any such ρ can be written in the form

$$\rho(\mathbf{x}) = \sum_{\mathbf{a}\in\mathcal{L}} \varphi(\mathbf{x}-\mathbf{a}) = (\varphi * \delta_{\mathcal{L}})(\mathbf{x}) \tag{3.2}$$

for some smooth, rapidly decaying function φ belonging to the Schwartz space $\mathcal{S}(\mathbb{R}^3)$, where $(f*g)(\mathbf{x})$ is the convolution $\int_{\mathbb{R}^3} f(\mathbf{x}-\mathbf{y})g(\mathbf{y})\,d\mathbf{y}$ and $\delta_{\mathcal{L}}(\mathbf{x}) = \sum_{\mathbf{a}\in\mathcal{L}} \delta(\mathbf{x}-\mathbf{a})$.

In the Von Laue condition, the reciprocal lattice of $\mathcal{L}$ will naturally emerge. The latter is defined by

$$\mathcal{L}' = \{\mathbf{k}\in\mathbb{R}^3 \,:\, \mathbf{k}\cdot\mathbf{a}\in 2\pi\mathbb{Z} \text{ for all } \mathbf{a}\in\mathcal{L}\}, \tag{3.3}$$

and is given in the case of (3.1) explicitly by $\mathcal{L}' = 2\pi A^{-T}\mathbb{Z}^3$, where A^{-T} denotes the transpose of the inverse of the matrix A. The Von Laue condition can now be stated as follows.

For simplicity, we only consider the square root of the intensity, i.e., up to trivial constants, the absolute value of the electric field (2.7). The latter, unlike its square, remains a well-defined mathematical object for infinitely extended systems, by interpreting it as a distributional Fourier transform. The powerful machinery of Fourier analysis then allows one to mathematically understand in a quick way the phenomenon of discrete diffraction patterns.

THEOREM 3.1 (Von Laue condition). *Let $\mathcal{L}$ be the Bravais lattice* (3.1)*, and let ρ_R be the electron density of a finite sample of diameter R of an $\mathcal{L}$-periodic crystal, i.e., $\rho_R(x) = \sum_{\mathbf{a}\in\mathcal{L},\,|\mathbf{a}|\le R}\varphi(\mathbf{x}-\mathbf{a})$ for some $\varphi\in\mathcal{S}(\mathbb{R}^3)$ (so that as $R\to\infty$, ρ_R approaches an $\mathcal{L}$-periodic density, represented in the form* (3.2)*). Assume that the incoming electric field is a plane wave $\mathbf{E}_0(\mathbf{y}) = \mathbf{n}\,e^{i\mathbf{k}_0\cdot\mathbf{y}}$ (see* (2.4)*), and the outgoing radiation is given by the electromagnetic model* (2.5)–(2.6) *with density ρ_R. Denote the corresponding intensity* (2.10) *by $I_R(\mathbf{x};\mathbf{k}_0)$. Assume, moreover, without loss of generality that $\mathbf{x}_c = 0$. Then*

$$\lim_{R\to\infty} (I_R(\mathbf{x};\mathbf{k}_0))^{1/2} = c_0\,\frac{(2\pi)^3}{|\det A|}\,\frac{1}{|\mathbf{x}|}\left|\mathbf{n} - \left(\tfrac{\mathbf{k}'(\mathbf{x})}{|\mathbf{k}'(\mathbf{x})|}\cdot\mathbf{n}\right)\tfrac{\mathbf{k}'(\mathbf{x})}{|\mathbf{k}'(\mathbf{x})|}\right| \sum_{\mathbf{a}'\in\mathcal{L}'} |\hat{\varphi}(\mathbf{a}')|\,\delta_{\mathbf{a}'}\left(\mathbf{k}'(\mathbf{x}) - \mathbf{k}_0\right), \tag{3.4}$$

where $\mathbf{k}'(\mathbf{x}) = \frac{\omega}{c}\frac{\mathbf{x}}{|\mathbf{x}|}$, $c_0 = (\frac{c\varepsilon_0}{2})^{1/2} c_{e\ell}$, and the convergence holds in the sense of distributions. In particular, the outgoing signal is zero unless the difference between outgoing and incoming wavevector, $\mathbf{k}'(\mathbf{x}) - \mathbf{k}_0$, is a reciprocal lattice vector.

For the simple diffraction model (2.11), analogous results for $I^{1/2}$ were presented in [St94, Fr07], and a rigorous treatment of the intensity I renormalized by volume was given in [Ho95]. The factor $\left|\mathbf{n} - \left(\frac{\mathbf{k}'(\mathbf{x})}{|\mathbf{k}'(\mathbf{x})|}\cdot\mathbf{n}\right)\frac{\mathbf{k}'(\mathbf{x})}{|\mathbf{k}'(\mathbf{x})|}\right|$, which reduces for real $\mathbf{n}$ to $|\sin(\angle(\mathbf{n},\mathbf{k}'(\mathbf{x})))|\,|\mathbf{n}|$, expresses the well-known fact—missed by the model (2.11)—that scattering along the polarization direction of the incoming X-ray beam is suppressed. We remark that the right-hand side of (3.4) makes rigorous sense (as a locally

bounded measure) via the standard definition of the delta function if considered as a function of the incoming wavevector $\mathbf{k}_0$ at fixed observation point $\mathbf{x}$, as implicitly assumed in the simple model (2.11). The meaning if considered as a function of $\mathbf{x}$ at fixed $\mathbf{k}_0$ is more complicated, due to the composition of the delta function with the nonlinear map $\mathbf{x} \mapsto \mathbf{k}'(\mathbf{x})$, and is not used here.

Proof. The central term in the outgoing field (2.7) is the structure factor $f_R(\mathbf{k}' - \mathbf{k}_0) = \widehat{\rho_R}(\mathbf{k}' - \mathbf{k}_0)$. As the sample diameter R gets large, ρ_R obviously converges weakly in the space $\mathcal{S}'(\mathbb{R}^3)$ of tempered distributions to the $\mathcal{L}$-periodic density ρ given by (3.2). By continuity of the Fourier transform under this convergence, $\widehat{\rho_R}(\cdot - \mathbf{k}_0)$ converges weakly in $\mathcal{S}'(\mathbb{R}^3)$ to the tempered distribution $\widehat{\rho}(\cdot - \mathbf{k}_0)$. By the generalized Poisson summation formula (see, e.g., [Fr07]), the Fourier transform of $\delta_{\mathcal{L}}$ is

$$\widehat{\delta_{\mathcal{L}}} = \frac{(2\pi)^3}{|\det A|}\delta_{\mathcal{L}'}, \tag{3.5}$$

with $\mathcal{L}'$ given by (3.3). The Fourier calculus rule $\widehat{f * g} = \hat{f}\,\hat{g}$ and the above convergences now give

$$\hat{\rho} = \frac{(2\pi)^3}{|\det A|}\hat{\varphi}\,\delta_{\mathcal{L}'}, \qquad \lim_{R\to\infty} f_R(\mathbf{k}'(\mathbf{x}) - \mathbf{k}_0) = \frac{(2\pi)^3}{|\det A|}\left(\hat{\varphi}\delta_{\mathcal{L}'}\right)(\mathbf{k}'(\mathbf{x}) - \mathbf{k}_0)\,.$$

Since the asymptotic expression for the structure factor is, by inspection, a locally bounded measure, its absolute value is well defined (see, e.g., [Di75]) and corresponds in the above case to replacing the factor $\hat{\varphi}$ by its absolute value. The result now follows immediately from (2.10) and the formula for $\mathbf{n}'(\mathbf{x})$ in (2.8). ∎

4. The design equations. We now have a second look at plane waves. Why are they the right radiation to use for the analysis of crystals?

Every researcher interested in X-ray diffraction is familiar with the Bragg/Von Laue phenomenon: the outgoing signal of a plane wave scattered at a crystal consists of sharp discrete peaks. But suppose plane waves were not given to us a priori, as the radiation emitted by conventional X-ray tubes. Would we know how to come up with them if our goal was to achieve a nice diffraction pattern? What, exactly, is the "connection" between a particular family of solutions to Maxwell's equations on the one hand and point sets with crystalline order on the other?

The connection is that plane waves and crystals have *matching symmetries*. By this we do not mean that they have the same symmetries. Plane waves have a larger, "continuous" family of symmetries. We first explain this informally, then make it precise in group-theoretical language, and then generalize beyond crystals.

Start with a crystal, i.e., a structure with atomic positions

$$\mathcal{S} = \{\mathbf{x}_0^{(\nu)} + \mathbf{a} \,:\, \mathbf{a} \in \mathcal{L},\ \nu = 1, \dots, M\},\ \ \mathcal{L} = \{i\mathbf{v}_1 + j\mathbf{v}_2 + k\mathbf{v}_3 \,:\, i, j, k \in \mathbb{Z}\} = A\,\mathbb{Z}^3, \tag{4.1}$$

where $\mathbf{x}_0^{(1)}, \dots, \mathbf{x}_0^{(m)}$ are the positions of finitely many reference atoms, $\mathbf{v}_1$, $\mathbf{v}_2$, $\mathbf{v}_3$ are linearly independent vectors in $\mathbb{R}^3$, and A is the matrix with columns given by these vectors. Thus the atom positions are obtained by translating finitely many reference atoms by each element of the lattice $\mathcal{L}$. Mathematically, this means that the crystal is the "orbit" of a finite set of points under a discrete group $\mathcal{L}$ of translations, and in particular that each element of $\mathcal{L}$ is a symmetry of the crystal, i.e., maps it to itself. The discrete translation group $\mathcal{L}$ is the *generating symmetry group* of the crystal.

We now look at plane waves,

$$\mathbf{E}_0(\mathbf{y}) = \mathbf{n}e^{i\mathbf{k}_0\cdot\mathbf{y}}, \quad \mathbf{n}\in\mathbb{C}^3, \quad \mathbf{k}_0\in\mathbb{R}^3, \quad \mathbf{k}_0\cdot\mathbf{n}=0. \tag{4.2}$$

Plane waves also have a translation symmetry. Their values at different positions just differ by phase factors,

$$\mathbf{E}_0(\mathbf{x}_0+\mathbf{a}) = (\text{phase factor depending on } \mathbf{a})\,\mathbf{E}_0(\mathbf{x}_0) \text{ for all } \mathbf{a}\in\mathbb{R}^3, \tag{4.3}$$

with

$$(\text{phase factor in (4.3)}) = e^{i\mathbf{k}_0\cdot\mathbf{a}}. \tag{4.4}$$

Mathematically, (4.3) means that the wave, a vector field on $\mathbb{R}^3$, is an "eigenfunction" of the operator which translates a vector field by a vector $\mathbf{a}\in\mathbb{R}^3$, $T_{-\mathbf{a}} : \mathbf{E}_0 \mapsto \mathbf{E}_0(\cdot+\mathbf{a})$. These operators form a continuous group which describes the action of the translation group $\mathcal{T}$ on vector fields. Hence plane waves are *simultaneous eigenfunctions of the continuous translation group* $\mathcal{T}$.

We now come to the interaction between wave and structure. The interaction occurs via the generalized structure factor (2.12) in the diffracted radiation field. Assume for simplicity that the density is a sum of delta functions at the atom positions, $\rho(y) = \sum_{\mathbf{a}\in\mathcal{L}} \delta_{\mathbf{x}_0+\mathbf{a}}(y)$. Then this factor is

$$\mathbf{f}_{\mathbf{E}_0}(\mathbf{k}') = \int_{\mathbb{R}^3} \mathbf{E}_0(\mathbf{y})\rho(\mathbf{y})e^{-i\mathbf{k}'\cdot\mathbf{y}}d\mathbf{y} = \sum_{\mathbf{a}\in\mathcal{L}} \mathbf{E}_0(\mathbf{x}_0+\mathbf{a})e^{-i\mathbf{k}'\cdot\mathbf{a}}. \tag{4.5}$$

The eigenfunction property (4.3) of the waves holds in particular for the crystalline translations $\mathbf{a}\in\mathcal{L}$, and so the structure factor reduces to a *phase factor sum*. The phase factors come from the symmetry of the wave. The points where they are evaluated come from the symmetry of the structure. And the sum "behaves nicely": it interferes constructively when $e^{-i(\mathbf{k}'-\mathbf{k}_0)\cdot\mathbf{a}} = 1$ for all $\mathbf{a}\in\mathcal{L}$, i.e., when $\mathbf{k}'-\mathbf{k}_0$ belongs to the reciprocal lattice $\mathcal{L}'$, and destructively otherwise.

To get constructive interference, it would be enough if the wave had just *the same* symmetry as the crystal, i.e. if (4.3)–(4.4) were true only for $\mathbf{a}$'s in the discrete translation group $\mathcal{L}$.[3] But to get destructive interference when the incoming radiation parameter $\mathbf{k}_0$ or the lattice parameters A are tuned off resonance, one needs (4.3)–(4.4) for all $\mathbf{a}$.

In summary, the discrete diffraction patterns of classical X-ray crystallography can be traced to the fact that crystals and plane waves have *matching symmetries*. Constructive interference comes from the fact that plane waves share the symmetry of crystals. Destructive interference comes from the fact that plane waves have a larger, continuous symmetry group.

Everything so far is just an abstract rationalization of a very well known phenomenon. But can it be generalized? The key is to realize that the foundation on which X-ray crystallography is built, the complex exponential form (4.2), can actually be *derived* from the innocent looking eigenvalue equation (4.3). If we combine two translations, $\mathbf{x}\mapsto(\mathbf{x}+\mathbf{a})\mapsto(\mathbf{x}+\mathbf{a})+\mathbf{b}$, we can either apply (4.3) to the whole translation, or separately to the two translations by $\mathbf{a}$ and $\mathbf{b}$, and so

$$(\text{phase factor at } \mathbf{a}+\mathbf{b}) = (\text{phase factor at } \mathbf{a})\cdot(\text{phase factor at } \mathbf{b}). \tag{4.6}$$

[3]This condition has infinite-dimensionally many solutions: it just means that the electric field multiplied by a complex exponential, $\mathbf{E}(\mathbf{x})e^{-i(\mathbf{k}'-\mathbf{k}_0)\cdot\mathbf{x}}$, shares the periodicity of the crystal. In the context of electron wavefunctions instead of electric fields, such waves are known as Bloch waves.

Mathematically, this means that the phase factor is a *group homomorphism* from the translation group to the multiplicative group $\mathbb{C}\backslash\{0\}$. And the only such group homomorphisms are the scalar complex exponentials (4.4)! Equation (4.4) together with (4.3) implies (2.4) (with polarization vector $\mathbf{n} = \mathbf{E}_0(\mathbf{x}_0)$), up to the orthogonality constraint on $\mathbf{n}$ and $\mathbf{k}_0$. The latter follows from Maxwell's equations, (2.2). So plane waves are those solutions to (4.3) which satisfy Maxwell. (See Theorem 5.1 for a precise statement.)

Thus we have a path from crystals to plane waves,

(4.7)

crystal $\longrightarrow$ generating symmetry group

$\longrightarrow$ continuous extension of symmetry group

$\longrightarrow$ eigenfunctions of continuous symmetry group which solve Maxwell.

This path can be generalized. We can start from any structure which is generated by a discrete isometry group, say a helical structure. The continuous extension of the group is then the helical group $\mathcal{H}_{\mathbf{e}}$ described in (6.1) below. Solving the resulting combined eigenfunction/Maxwell problem will yield twisted waves.

The noncrystalline but highly symmetric structures which are generated by *some* discrete isometry group form an interesting class. This class was recently introduced and studied by one of us [Ja06], and has been named *objective structures*. Like crystals, objective structures can be completely classified [DEJ].

The remarkable constructive/destructive interference properties of the structure factor (4.5) survive as long as the generating symmetry group of the structure is abelian. Here we can rely on a far-reaching generalization of the Poisson summation formula due to Weil [We64] (see section 8). We note that Weil had a completely different motivation, number theory rather than molecular biology.

To conclude this section, we formulate the design problem suggested by the path (4.7) precisely. Translations are a special case of isometries of three-dimensional space. The Euclidean group $E(3)$ of isometries consists of the elements $g = (\mathbf{R}|\mathbf{c})$ acting on points in $\mathbb{R}^3$ according to the rule $g(\mathbf{x}) = \mathbf{R}\mathbf{x} + \mathbf{c}$, where $\mathbf{R}$ is any orthogonal 3×3 matrix and $\mathbf{c} \in \mathbb{R}^3$. The natural action on vector fields $\mathbf{E} : \mathbb{R}^3 \to \mathbb{C}^3$ is

$$((\mathbf{R}|\mathbf{c})\mathbf{E})(\mathbf{x}) = \mathbf{R}\mathbf{E}\left(\mathbf{R}^{-1}(\mathbf{x} - \mathbf{c})\right). \tag{4.8}$$

Note that $\mathbf{R}^{-1}(\cdot - c)$ is the inverse element $(\mathbf{R}|\mathbf{c})^{-1}$. The translation symmetry (4.3) of plane waves has a natural analogue for any closed subgroup G of the Euclidean group $E(3)$, namely that

$$(g\mathbf{E}_0)(\mathbf{x}) = \chi_g \mathbf{E}_0(\mathbf{x}) \text{ for some complex number } \chi_g \text{ and all } g \text{ in } G. \tag{4.9}$$

Equation (4.9) *together with* (2.2) *are our design equations.* In words, the incoming radiation is simultaneously an eigenfunction of the group (with eigenvalues χ_g) and a divergence-free eigenfunction of the Laplacian (with eigenvalue $-\omega^2/c^2$). Typically, G—the "desired symmetry of the radiation"—is obtained as a continuous extension $G \supset G_0$ of a discrete subgroup G_0 of $E(3)$—the "generating symmetry of a structure".

Note that the transformed field $g\mathbf{E}_0$ (left-hand side in (4.9)) reduces to the left-hand side of (4.3) when the group element g is given by the translation $(\mathbf{I}| - \mathbf{a})$.

In the next two sections, we will solve the design equations for some interesting examples. We will make use of the fact that as for (4.3), the eigenvalue $\chi(g)$ as a function of g must be a group homomorphism.

LEMMA 4.1 (character lemma). *If* $\mathbf{E}_0$ *is any solution to the design equations* (2.2), (4.9) *for the group* G *which is not identically zero, then the function* $\chi : G \to \mathbb{C}$ *in* (4.9) *is a bounded continuous group homomorphism from* G *to the multiplicative group* $\mathbb{C}\backslash\{0\}$.

Proof. The argument is the same as that leading to (4.6). Equation (4.9) shows that for g_1, $g_2 \in G$,

$$\chi(g_1 g_2)\mathbf{E}_0 = (g_1 g_2)\mathbf{E}_0 = g_1(g_2\mathbf{E}_0) = \chi(g_1)g_2\mathbf{E}_0 = \chi(g_1)\chi(g_2)\mathbf{E}_0. \tag{4.10}$$

Evaluation at a point $\mathbf{x}$ where $\mathbf{E}_0$ is not zero shows that χ is a group homomorphism. Boundedness and continuity of χ are a direct consequence of the same properties for $\mathbf{E}_0$. ∎

In the case when G is abelian, the bounded continuous group homomorphisms to $\mathbb{C}\backslash\{0\}$ are called the *characters* of G. The group of characters

$$G' := \{\chi : G \to \mathbb{C}\backslash\{0\} : \chi \text{ is a character of } G\} \tag{4.11}$$

is called the *dual group* of G and satisfies the reflexivity relation $(G')' \cong G$.

As will become clear after having discussed some examples, the dual group G' can be interpreted physically as a space of scalar "waves" on the group or equivalently a "wavevector space" which parameterizes the radiation that solves the design equations, just as the wavevectors $\mathbf{k}_0$ in (4.2) parameterize plane waves.

Finally we remark that the design equation (4.9) is intrinsically abelian and should really only be used for abelian G. Namely, (4.11) shows that the action of G on simultaneous eigenfunctions must be abelian, $(g_1 g_2)\mathbf{E}_0 = (g_2 g_1)\mathbf{E}_0$, since the right-hand side in (4.10) is independent of the order of the g_i.

For non-abelian but compact subgroups G of $E(3)$, a generalization of the design equations which can yield radiation families on which G acts in a non-abelian way has been worked out by one of us, and will be presented elsewhere. This may be of interest to analyze structures such as buckyballs and icosahedral viruses [CK62], which are generated by non-abelian discrete symmetries. In this case one can appeal to representation theory of groups. The set of characters of G is no longer given by (4.11), and has the structure of a hypergroup [La15] instead of a group.

5. Plane waves as solution to the design equations. After having formalized our design criterion for structure-adapted radiation into a set of equations, we can state our insight from section 4 that plane waves are right for crystals as a mathematical theorem.

THEOREM 5.1 (plane waves are right for crystals). *Let* G *be the translation group*

$$\mathcal{T} = \{(\mathbf{I}|\mathbf{c}) : \mathbf{c} \in \mathbb{R}^3\}, \quad \mathbf{x} \mapsto \mathbf{x} + \mathbf{c}. \tag{5.1}$$

Then the solutions to the design equations ((2.2), (4.9)*) are precisely the plane waves*

$$\mathbf{E}_0(\mathbf{x}) = \mathbf{n}\, e^{i\mathbf{k}_0 \cdot \mathbf{x}}, \quad \mathbf{k}_0 \in \mathbb{R}^3, \quad \mathbf{n} \in \mathbb{C}^3, \quad \mathbf{k}_0 \cdot \mathbf{n} = 0. \tag{5.2}$$

Proof. By the character lemma, the function $\chi : G \to \mathbb{C}$ in (4.9) must be a character of $\mathcal{T}$. The characters are well known to be given by

$$\chi_{\mathbf{k}}(\mathbf{a}) = e^{i\mathbf{k}\cdot\mathbf{a}}, \quad \mathbf{k} \in \mathbb{R}^3. \tag{5.3}$$

Fix $\mathbf{k}_0 \in \mathbb{R}^3$, and consider the character $\chi_{-\mathbf{k}_0}$. The design equation (4.9) says that

$$\mathbf{E}_0(\cdot - \mathbf{a}) = e^{i(-\mathbf{k}_0)\cdot\mathbf{a}}\mathbf{E}_0 \quad \text{for all } \mathbf{a} \in \mathbb{R}^3.$$

Evaluation at $\mathbf{x} = \mathbf{a}$ gives $\mathbf{E}_0(0) = e^{-i\mathbf{k}_0\cdot\mathbf{x}}\mathbf{E}_0(\mathbf{x})$, that is, $\mathbf{E}_0$ is of form $\mathbf{n}e^{i\mathbf{k}_0\cdot\mathbf{x}}$ with $\mathbf{n} = \mathbf{E}_0(0)$. The first of the Maxwell equations in (2.2) holds automatically. The second one holds if and only if $\mathbf{k}_0 \cdot \mathbf{E}_0(0) = 0$. This completes the proof. ∎

The proof says that fixing a wavevector $\mathbf{k}_0$ corresponds precisely to fixing a character $\chi : G \to \mathbb{C}$ in the symmetry condition (4.9). For each fixed character, the solutions of the design equations form a complex vector space parameterized by $\{\mathbf{n} \in \mathbb{C}^3 : \mathbf{k}_0 \cdot \mathbf{n} = 0\}$. This vector space has dimension 2, except in the special case $\chi = 1$, where the dimension is 3.

6. Twisted waves. We now look at the case when G is the helical group

$$\mathcal{H}_{\mathbf{e}} = \{(\mathbf{R}_\theta|\tau\mathbf{e}) : \theta \in [0, 2\pi),\, \tau \in \mathbb{R}\},\quad \mathbf{R}_\theta = \begin{pmatrix} \cos\theta & -\sin\theta & 0 \\ \sin\theta & \cos\theta & 0 \\ 0 & 0 & 1 \end{pmatrix}, \tag{6.1}$$

where $\mathbf{e}$ is a given unit vector in $\mathbb{R}^3$, τ is the amount of displacement along $\mathbf{e}$, and $\mathbf{R}_\theta$ is the rotation about $\mathbf{e}$ by the angle θ. The above matrix representation of $\mathbf{R}_\theta$ corresponds to a cartesian coordinate system in which the third coordinate direction is given by $\mathbf{e}$.

This group naturally arises as the continuous extension of any discrete generating symmetry group of a helix or nanotube structure.

It will be convenient to work in cylindrical coordinates with respect to the helical axis, that is,

$$\mathbf{e} = \mathbf{e}_3 = \begin{pmatrix} 0 \\ 0 \\ 1 \end{pmatrix},\quad \mathbf{x} = \begin{pmatrix} x_1 \\ x_2 \\ x_3 \end{pmatrix} = \begin{pmatrix} r\cos\varphi \\ r\sin\varphi \\ z \end{pmatrix},\quad r \in [0,\infty),\, \varphi \in [0, 2\pi),\, z \in \mathbb{R}. \tag{6.2}$$

In cylindrical coordinates, the action (4.8) of the helical group (6.1) on vector fields assumes the following simple form:

$$\Big((\mathbf{R}_\theta|\tau\mathbf{e})\mathbf{E}\Big)(r, \varphi, z) = \mathbf{R}_\theta\mathbf{E}(r, \varphi - \theta, z - \tau). \tag{6.3}$$

See Figure 3. Here and below, $\mathbf{E}$ is a function from polar coordinate space to the cartesian space $\mathbb{R}^3$; that is, E_1, E_2, E_3 are the cartesian field components of $\mathbf{E}$, and the action of the group on the direction of the field vectors is the usual action of the 3×3 matrix $\mathbf{R}_\theta$ on vectors.

THEOREM 6.1 (twisted waves). *Let G be the helical group $\mathcal{H}_{\mathbf{e}}$ with axis $\mathbf{e}$. Then the solutions to the design equations ((4.9), (2.2)) are precisely*

$$\mathbf{E}_0(r, \varphi, z) = e^{i(\alpha\varphi + \beta z)}\, \mathbf{R}_\varphi\, \mathbf{N}(\mathbf{n}) \begin{pmatrix} J_{\alpha+1}(\gamma r) \\ J_{\alpha-1}(\gamma r) \\ J_\alpha(\gamma r) \end{pmatrix}, \tag{6.4}$$

with $(\alpha, \beta, \gamma) \in \mathbb{Z} \times \mathbb{R} \times (0, \infty)$ ("parameter vector"), $\mathbf{n} \in \mathbb{C}^3$ ("polarization vector"), and

$$(0, \gamma, \beta) \cdot \mathbf{n} = 0. \tag{6.5}$$

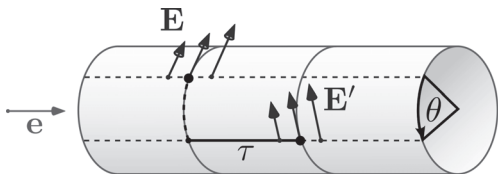

FIG. 3. *Action of the helical group on vector fields and design of twisted waves. Start from a given vector field* $\mathbf{E}$*. The transformed field* $\mathbf{E}'$ *(right-hand side of* (6.3)*) under the action of a typical element of the helical group is obtained as follows:* (i) *translate the base points along the helical axis* $\mathbf{e}$ *by some amount* τ *while leaving the field direction unchanged;* (ii) *rotate the base points by some angle* θ*; and* (iii) *rotate the field direction by the same angle. The design equations require that the transformed field only differs from the original field by a phase factor, regardless of how* τ *and* θ *are chosen. Time-harmonic electric fields with this property are named twisted waves and can be proven to have the mathematical form* (6.4) *(see Theorem* 6.1*).*

Here $\mathbf{N}(\mathbf{n})$ *is a certain* 3×3 *matrix ("polarization tensor") which depends linearly on the polarization vector* $\mathbf{n}$*,*

$$\mathbf{N}(\mathbf{n}) = \begin{pmatrix} \frac{n_1+in_2}{2} & \frac{n_1-in_2}{2} & 0 \\ \frac{n_2-in_1}{2} & \frac{n_2+in_1}{2} & 0 \\ 0 & 0 & n_3 \end{pmatrix}, \tag{6.6}$$

the J_α *are Bessel functions,* (r,φ,z) *are cylindrical coordinates* (6.2) *with respect to the helical axis, and* $\mathbf{E}_0$ *is the cartesian field vector. The associated frequency in the design equations is given by* $\omega = c|(0,\gamma,\beta)|$*.*

We call the electric fields (6.4)–(6.6) *twisted waves.* Figure 1 in the introduction shows the twisted wave with parameter vector $(\alpha,\beta,\gamma) = (5,3,1)$ and polarization vector $\mathbf{n} = (1,0,0)$.

Substituting the elementary identity (6.18) into (6.4) yields the following alternative representation of twisted waves in terms of separated solutions to the Helmholtz equation:

$$\mathbf{E}_0(r,\varphi,z) = \mathbf{n}_+ e^{i((\alpha+1)\varphi+\beta z)} J_{\alpha+1}(\gamma r) + \mathbf{n}_- e^{i((\alpha-1)\varphi+\beta z)} J_{\alpha-1}(\gamma r) + \mathbf{n}_0 e^{i(\alpha\varphi+\beta z)} J_\alpha(\gamma r), \tag{6.7}$$

where $\mathbf{n}_+$, $\mathbf{n}_-$, and $\mathbf{n}_0$ are the columns of the polarization tensor $\mathbf{N}(\mathbf{n})$ in (6.6). Note that the three contributions in (6.7) are not themselves solutions to Maxwell's equations, because only their sum is divergence-free.

The parameters α and β can be interpreted as eigenvalues of angular momentum and momentum. Namely, it is easily checked that the twisted wave (6.4), (6.6) is an exact solution to the eigenvalue equations

$$J_z\mathbf{E}_0 = \alpha\,\mathbf{E}_0, \quad P_z\mathbf{E}_0 = \beta\,\mathbf{E}_0, \quad \text{where } J_z = \frac{1}{i}\frac{\partial}{\partial\varphi} + \begin{pmatrix} 0 & -i & \\ i & 0 & \\ & & 0 \end{pmatrix}, \quad P_z = \frac{1}{i}\frac{\partial}{\partial z}. \tag{6.8}$$

Here P_z is the well-known quantum mechanical momentum operator in the axial direction, and J_z is the correctly defined angular momentum operator on vector fields with respect to the helical axis (whose cartesian form (6.9) can be found in [CT97]). These operators arise in our context of classical electrodynamics as the infinitesimal generators of the action (4.8) of the rotational and translational subgroup of the helical

group (6.1) on vector fields: in cartesian coordinates,

$$\frac{d}{d\theta}\mathbf{R}_\theta \mathbf{E}(\mathbf{R}_\theta^{-1}\mathbf{x})\Big|_{\theta=0} = \Big(-\mathbf{e}\cdot(\mathbf{x}\wedge\nabla) + \mathbf{e}\wedge\Big)\mathbf{E}(\mathbf{x}) = \frac{1}{i}(J_z\mathbf{E})(\mathbf{x}), \tag{6.9}$$

$$\frac{d}{d\tau}\mathbf{E}(\mathbf{x}-\tau\mathbf{e})\Big|_{\tau=0} = -(\mathbf{e}\cdot\nabla)\mathbf{E}(\mathbf{x}) = \frac{1}{i}(P_z\mathbf{E})(\mathbf{x}). \tag{6.10}$$

We remark that the eigenvalue equations (6.8) are equivalent to the design equation (4.9) with character $\chi(\theta,\tau) = e^{-i(\alpha\theta+\beta\tau)}$.

Proof. First we exploit the symmetry condition. By the character lemma, the function χ in (4.9) must be a character of the helical group $\mathcal{H}_\mathbf{e}$. It is clear from the parameterization (6.1) that the helical group $\mathcal{H}_\mathbf{e}$ is isomorphic to $S^1\times\mathbb{R}$, where $S^1 \cong [0,2\pi)$ with the usual addition of angles modulo 2π. The characters $\chi : S^1\times\mathbb{R}\to\mathbb{C}\backslash\{0\}$ of $S^1\times\mathbb{R}$ are well known to be

$$\chi_{\alpha,\beta}(\theta,\tau) = e^{i(\alpha\theta+\beta\tau)}, \quad (\alpha,\beta)\in\mathbb{Z}\times\mathbb{R}. \tag{6.11}$$

In particular, the dual group (4.11) is given by $(\mathcal{H}_\mathbf{e})' \cong \mathbb{Z}\times\mathbb{R}$. Fix $(\alpha,\beta)\in\mathbb{Z}\times\mathbb{R}$, and consider the character $\chi_{-(\alpha,\beta)} : S^1\times\mathbb{R}\to\mathbb{C}\backslash\{0\}$. The first design equation, (4.9), says that $\mathbf{R}_\theta\mathbf{E}_0(r,\varphi-\theta,z-\tau) = e^{i(-\alpha\varphi-\beta\tau)}\mathbf{E}_0(r,\varphi,z)$. Evaluation at $\varphi=\theta$, $z=\tau$ gives

$$\mathbf{E}_0(r,\varphi,z) = e^{i(\alpha\varphi+\beta z)}\mathbf{R}_\varphi\mathbf{E}_0(r,0,0). \tag{6.12}$$

Now we exploit the Helmholtz equation (first equation in (2.2)). Substituting the ansatz (6.12) into this equation gives three coupled ordinary differential equations (ODEs) for $\mathbf{E}_0(r,0,0)$. These ODEs can be decoupled by simultaneously diagonalizing the matrices $\mathbf{R}_\varphi$, $\varphi\in[0,2\pi)$, with a unitary transformation. Simultaneous diagonalization is possible because the group $SO(2)$ of these matrices is *abelian*. We have

$$\mathbf{R}_\varphi = U\begin{pmatrix} e^{i\varphi} & & \\ & e^{-i\varphi} & \\ & & 1\end{pmatrix}U^{-1} \text{ for all } \varphi\in[0,2\pi), \text{ with } U = \begin{pmatrix} \frac{i}{\sqrt{2}} & \frac{-i}{\sqrt{2}} & 0\\ \frac{1}{\sqrt{2}} & \frac{1}{\sqrt{2}} & 0\\ 0 & 0 & 1\end{pmatrix}. \tag{6.13}$$

Let $\tilde{\mathbf{E}}(r,\varphi,z) := U^{-1}\mathbf{E}_0(r,\varphi,z)$. Using the notation $\sigma_1=1$, $\sigma_2=-1$, $\sigma_3=0$, we have that $\tilde{E}_j(r,\varphi,z) = e^{i((\alpha+\sigma_j)\varphi+\beta z)}\tilde{E}_j(r,0,0)$. Since the Helmholtz equation is invariant under the transformation $\mathbf{E}_0\mapsto\tilde{\mathbf{E}} = U^{-1}\mathbf{E}_0$, we can substitute $\tilde{\mathbf{E}}$ into this equation and obtain, using that the Laplacian in cylindrical coordinates is $\Delta = \partial^2/\partial r^2 + \frac{1}{r}\partial/\partial r + \partial^2/\partial\varphi^2 + \partial^2/\partial z^2$, the following ODE for the components:

$$\left(\frac{\partial^2}{\partial r^2} + \frac{1}{r}\frac{\partial}{\partial r} - \frac{(\alpha+\sigma_j)^2}{r^2} + \big((\tfrac{\omega}{c})^2-\beta^2\big)\right)\tilde{E}_j(r,0,0) = 0, \quad j=1,2,3. \tag{6.14}$$

That is, the radial functions $\tilde{E}_j(r,0,0)$ are solutions to Bessel's equation. Boundedness of $\tilde{E}_j$ implies that we must have $(\omega/c)^2-\beta^2\geq 0$. Moreover, for integer values of α there is only a one-dimensional space of bounded solutions, given by

$$\tilde{E}_j(r,0,0) = c_j J_{\alpha+\sigma_j}(\gamma r), \quad \gamma = \sqrt{(\tfrac{\omega}{c})^2 - \beta^2}, \quad c_j \in \mathbb{C}. \tag{6.15}$$

For reasons that will emerge later, it is fruitful to parameterize the solution space not by $\mathbf{c} \in \mathbb{C}^3$ but by $\mathbf{n} := U\mathbf{c}$. It follows that

$$\mathbf{E}_0(r,0,0) = \mathbf{N}(\mathbf{n}) \begin{pmatrix} J_{\alpha+1}(\gamma r) \\ J_{\alpha-1}(\gamma r) \\ J_\alpha(\gamma r) \end{pmatrix}, \quad \mathbf{n} \in \mathbb{C}^3, \quad \mathbf{N}(\mathbf{n}) := U \operatorname{diag}(U^{-1}\mathbf{n}). \tag{6.16}$$

Here and below, $\operatorname{diag}(\mathbf{c})$ denotes the diagonal matrix whose diagonal entries are given by the components of the vector $\mathbf{c}$. Using (6.13), it is easy to check that the 3×3 matrix $\mathbf{N}(\mathbf{n})$ introduced above is given by the expression in the theorem. Substitution into (6.12) shows that $\mathbf{E}_0$ has the form (6.4), except that $\mathbf{n} \in \mathbb{C}^3$ is still arbitrary.

It remains to analyze the second Maxwell equation, $\operatorname{div} \mathbf{E}_0 = 0$. A lengthy calculation (included for the convenience of the reader in the supplementary material (M104341_01.pdf [local/web 246KB])) shows that the field given by (6.12), (6.16) satisfies

$$\operatorname{div} \mathbf{E}_0 = i\,((0,\gamma,\beta)\cdot\mathbf{n})\; e^{i(\alpha\varphi+\beta z)} J_\alpha(\gamma r). \tag{6.17}$$

In particular, we see that the field is divergence-free if and only if (6.5) holds. This completes the proof of Theorem 6.1. ∎

Next we present an interesting algebraic property of the somewhat mysterious polarization tensor which emerged from the above proof.

LEMMA 6.2 (intertwining lemma). *The polarization tensor* $\mathbf{N}(\mathbf{n})$ *introduced in* (6.16) *satisfies*

$$\mathbf{R}_\varphi \mathbf{N}(\mathbf{n}) = \mathbf{N}(\mathbf{n}) \begin{pmatrix} e^{i\varphi} & & \\ & e^{-i\varphi} & \\ & & 1 \end{pmatrix} \quad \textit{for all } \mathbf{n} \in \mathbb{C}^3. \tag{6.18}$$

Equation (6.18) means that $\mathbf{N}(\mathbf{n})$ "intertwines" the standard representation and the diagonal representation of the rotational subgroup $SO(2)$ of the helical group $\mathcal{H}_\mathbf{e}$ on $\mathbb{C}^3$.

Proof. By the diagonal representation (6.13) of $\mathbf{R}_\varphi$ and the fact that diagonal matrices commute, we have, abbreviating the diagonal matrix in the lemma by D_φ,

$$\mathbf{R}_\varphi \mathbf{N}(\mathbf{n}) = U\, D_\varphi U^{-1} \mathbf{N}(\mathbf{n}) = U\, D_\varphi \operatorname{diag}(U^{-1}\mathbf{n}) = U \operatorname{diag}(U^{-1}\mathbf{n}) D_\varphi = \mathbf{N}(\mathbf{n})\, D_\varphi. \quad ∎$$

Next we compute the magnetic field associated with a twisted wave. We use the cylindrical components of the wave and apply the formula for the curl of a vector field $\mathbf{v}$ in cylindrical coordinates given in the supplementary material. After some calculation we find that

$$\operatorname{curl} \mathbf{E}_0 = e^{i(\alpha\varphi+\beta z)} \mathbf{R}_\varphi \mathbf{N}(i\mathbf{k}_0 \times \mathbf{n}) \begin{pmatrix} J_{\alpha+1}(\gamma r) \\ J_{\alpha-1}(\gamma r) \\ J_\alpha(\gamma r) \end{pmatrix}, \quad \mathbf{k}_0 := \begin{pmatrix} 0 \\ \gamma \\ \beta \end{pmatrix}. \tag{6.19}$$

That is, to obtain the curl one just has to replace the vector $\mathbf{n}$ inside the polarization tensor by $i\mathbf{k}_0 \times \mathbf{n}$.

The magnetic field associated with the twisted wave (6.4) can be immediately read off from (2.3) and (6.19):

$$\mathbf{B}_0(r,\varphi,z) = e^{i(\alpha\varphi+\beta z)}\,\mathbf{R}_\varphi\,\mathbf{N}(\tfrac{1}{\omega}\mathbf{k}_0\times\mathbf{n})\begin{pmatrix} J_{\alpha+1}(\gamma r)\\ J_{\alpha-1}(\gamma r)\\ J_\alpha(\gamma r)\end{pmatrix},\quad \text{with } \mathbf{k}_0 \text{ as in (6.19).} \tag{6.20}$$

Hence for twisted waves, with the "right" definition of wavevector, the map from $\mathbf{E}_0$ to $\mathbf{B}_0$ is precisely the same map on the polarization vector $\mathbf{n}$ as for plane waves (2.4).

A deeper understanding of this fact, and of the related formula (6.17) for the divergence, can be achieved from the Fourier decomposition of twisted waves which can be derived via the Bessel integral $J_\alpha(A) = \frac{1}{2\pi}\int_0^{2\pi} e^{i(\alpha\varphi' - A\sin\varphi')}d\varphi'$ (see the supplementary material for details and visualization):

$$\mathbf{E}_0(\mathbf{x}) = \frac{1}{2\pi}\int_0^{2\pi}\Big(e^{i\alpha\Phi}\mathbf{R}_\Phi\mathbf{n}\Big)e^{i\mathbf{R}_\Phi\mathbf{k}_0\cdot\mathbf{x}}d\Phi. \tag{6.21}$$

Formula (6.21) has an interesting alternative interpretation, namely as a *group average* instead of a $\mathbf{k}$-space integral. Letting $\mathbf{E}_{plane}(\mathbf{x})$ denote the plane wave $\mathbf{n}\,e^{i\mathbf{k}_0\cdot\mathbf{x}}$, one has

$$\mathbf{E}_0(\mathbf{x}) = \int_G \chi_\alpha(g)\Big(g\mathbf{E}_{plane}\Big)(\mathbf{x})\,d\mu(g), \tag{6.22}$$

where G is the group of rotations around the cylindrical axis, $\chi_\alpha(g) = e^{i\alpha\varphi}$ is a character of the group, and $d\mu = \frac{1}{2\pi}d\Phi$ is the Haar measure on the group. This shows that a twisted wave is *an integral of the image of a plane wave under the group of rotations about a fixed axis against a character*. The polarization vector $\mathbf{n}$ and the "cartesian reduced wavevector" $(0,\gamma,\beta)$ are just the polarization vector and the wavevector of this plane wave; the angular wavenumber α comes from the character.

Expression (6.22) is an example of a *Wigner projection*, a concept first introduced in the context of quantum systems in [Wi31]. It is clear that (6.22) yields a solution to the design equations (4.9), (2.2): first, it implies by an elementary change of variables that for any $h\in G$, $h\mathbf{E}_0 = \chi_{-\alpha}(h)\mathbf{E}_0$; and second, it satisfies (2.2), since the group action (4.8) maps solutions to Maxwell's equations again to solutions. This approach allows one to construct solutions to the design equations for general abelian isometry groups [Ju16], but the remarkable fact that in the helical case Wigner-projecting plane waves already gives *all* solutions does not follow from the above considerations.

7. The reciprocal lattice of a helical structure. Helical structures are orbits of a finite set of atoms under a discrete subgroup of the helical group. For these structures, in the context of X-ray fiber diffraction a notion of "reciprocal helical lattice" has been introduced by Klug, Crick, and Wyckoff [KCW58], by periodically extending the helical subgroup to a Bravais lattice in $\mathbb{R}^2$ and applying the concept of reciprocal Bravais lattice. We show here that this notion of reciprocal helical lattice has an *intrinsic group-theoretic meaning* which parallels, rather than needs to rely on, that of the reciprocal lattice in the crystal case. The reciprocal helical lattice and its group-theoretic meaning emerge naturally from the diffraction patterns of helical structures subjected to *twisted waves*; see the following section.

The atomic positions in a helical structure are of the form

$$\mathcal{S} = \{g\,\mathbf{x}_0^{(\nu)} \,:\, g\in H_0,\, \nu = 1,\dots,M\}, \tag{7.1}$$

where $\mathbf{x}_0^{(1)}, \ldots, \mathbf{x}_0^{(M)}$ are the atomic positions of a reference molecule and H_0 is a *discrete helical group*, by which we mean a discrete subgroup of the helical group $\mathcal{H}_\mathbf{e}$ with axis $\mathbf{e}$ (see (6.1)) of the form

$$H_0 = \{g_0^i h_0^j \,:\, i \in \mathbb{Z},\, j = 1, \ldots, n\}, \quad h_0 = (\mathbf{R}_{\theta_0}|\tau_0\mathbf{e}),\; g_0 = (\mathbf{R}_{2\pi/n}|0), \tag{7.2}$$

with $\theta_0 \in [0, 2\pi)$, $\tau_0 \in \mathbb{R}$, $\tau_0 \neq 0$, and $n \in \mathbb{N}$.

Alternatively, we can describe the group (7.2) by a parameter space $\mathcal{H}_0$, called the *helical lattice*, which parameterizes the group elements by their rotation angle and translation parameter,

$$\begin{aligned} H_0 &= \left\{(\mathbf{R}_\theta|\tau\mathbf{e}) \,:\, \begin{pmatrix}\theta\\ \tau\end{pmatrix} \in \mathcal{H}_0\right\}, \\ \mathcal{H}_0 &= \left\{i\begin{pmatrix}\frac{2\pi}{n}\\ 0\end{pmatrix} + j\begin{pmatrix}\theta_0\\ \tau_0\end{pmatrix} \bmod \begin{pmatrix}2\pi\\ 0\end{pmatrix} \,:\, i, j \in \mathbb{Z}\right\} = \underbrace{\begin{pmatrix}\frac{2\pi}{n} & \theta_0\\ 0 & \tau_0\end{pmatrix}}_{=:A} \mathbb{Z}_n \times \mathbb{Z} \bmod \begin{pmatrix}2\pi\\ 0\end{pmatrix}. \end{aligned} \tag{7.3}$$

Here $v \bmod (2\pi, 0)$ denotes the unique vector in $[0, 2\pi) \times \mathbb{R}$ which differs from v by an integer multiple of $(2\pi, 0)$. See Figure 4. In case $n = 1$ and $M = 1$, g_0 is the identity and $\mathcal{S}$ is a helix. When $n = 1$ and $M > 1$, g_0 is the identity and $\mathcal{S}$ a "molecular helix," built from identical copies of a reference molecule with M atoms. In case $n > 1$, $\mathcal{S}$ is the union of n identical helices, basic examples being "zigzag" or "armchair" carbon nanotubes. The parameters τ_0 and θ_0 of the generating screw displacement h_0 encode the pitch p and the number q of subunits per turn of the helices. The pitch is defined as the axial displacement for one full rotation. $p = 2\pi\tau_0/\theta_0$, and the number of subunits (i.e., rotated and translated copies of the set $\{\mathbf{x}_0^{(1)}, \ldots, \mathbf{x}_0^{(M)}\}$) per turn is $q = 2\pi/\theta_0$. In physical and biological examples, the latter number is typically a rational number but not an integer.

Example 1 (carbon nanotubes). Carbon nanotubes of all chiralities are of the form (7.1), (7.3). For the single-walled (n', m') nanotube, $M = 2$ and $n = \gcd(n', m')$. To give a specific example, single-walled (6,5) carbon nanotubes with axis $\mathbf{e} = (0, 0, 1)$ correspond to $M = 2$ (two atoms per unit cell), $n = 1$ (single helix),

$$\theta_0 = \frac{149}{182}\,2\pi, \quad \tau_0 = \frac{3}{2\sqrt{91}}\,\ell \;\text{ with } \ell = 1.43\,A^o \text{ (C-C bond length)},$$

$$\mathbf{x}^{(1)} = (r, 0, 0), \text{ where } r = \frac{\sqrt{3}\sqrt{91}}{2\pi}\,\ell \text{ (nanotube radius)}, \quad \mathbf{x}^{(2)} = (\mathbf{R}_{\theta_0/3}|\tfrac{\tau}{3}\mathbf{e})\,\mathbf{x}^{(1)}.$$

Example 2 (tobacco mosaic virus (TMV)). This is a basic example of a filamentous virus, built from a single protein. The protein molecules are arranged in a low-pitch helix, with $16\frac{1}{3}$ proteins per turn and with adjacent turns in contact. The parameter values in (7.1), (7.3) are $M = 1284$ (number of atoms in the protein), $n = 1$ (single helix), and

$$\theta_0 = \frac{2\pi}{16\frac{1}{3}} = \frac{3}{49}\,2\pi, \quad \tau_0 = 1.402\,A^o.$$

The values for θ_0 and τ_0, taken from [GZ11], correspond to the low-calcium state.

The groups in (7.3) are not some ad hoc ansatz. It can be shown that they are the *lattice subgroups* of the helical group (6.1), whereas the Bravais lattices are the

lattice subgroups of the translation group (5.1).[4]

We now introduce a purely group-theoretical notion of reciprocal lattice. We first state this notion in abstract mathematical language and then show how it reduces to familiar concepts in the crystalline and helical case.

DEFINITION 7.1 (reciprocal lattice group). *Let H_0 be a lattice subgroup of the helical group (see* (7.3)*), or more generally any lattice subgroup of a locally compact abelian group H. Recall from* (4.11) *the dual group of H, $H' = \{\chi : H \to \mathbb{C}\backslash\{0\} : \chi$ is a character of $H\}$. The* reciprocal lattice group *of H_0 with respect to H is the set of those characters of H which are equal to* 1 *on H_0, i.e.,*

$$H_0' = \{\chi \in H' : \chi(h) = 1 \text{ for all } h \in H_0\}.$$

Thus the reciprocal lattice group H_0' is a subgroup of the dual group H'. In group theory, H_0' is a well-known object, called the annihilator of H_0 [HR63] or the orthogonal group of H_0 with respect to H [RS00]; the latter terminology views the equation $\chi(h) = 1$ as analogous to the vanishing of a proper inner product between elements χ and h of some vector space.

Physically, the dual group consists of certain scalar waves on the group or equivalently of the wavevectors parameterizing them, and the reciprocal lattice group consists of resonant scalar waves on the group or the corresponding resonant wavevectors. Table 1 below gives their explicit form in the crystalline and helical cases.

TABLE 1

The symmetry groups associated with crystals and helical structures. The ambient isometry group, lattice subgroup, and reciprocal lattice group govern, respectively, the radiation, the structure, and the diffraction pattern.

	Crystals	Helical structures
Ambient isometry group H	Translations $\{(\mathbf{I}\|\mathbf{a}) : \mathbf{a} \in \mathbb{R}^d\}$	Screw displacements $\{(\mathbf{R}_\theta\|\tau\mathbf{e}) : \theta \in [0, 2\pi), \tau \in \mathbb{R}\}$
lattice subgroup H_0	$\{(\mathbf{I}\|\mathbf{a}) : \mathbf{a} \in A\mathbb{Z}^d\}$, A invertible $d \times d$ matrix	$\left\{(\mathbf{R}_\theta\|\tau\mathbf{e}) : \begin{pmatrix}\theta\\ \tau\end{pmatrix} \in A\mathbb{Z}_n \times \mathbb{Z} \bmod \begin{pmatrix}2\pi\\ 0\end{pmatrix}\right\}$, A invertible 2×2 matrix of form (7.3)
parameter space $\mathcal{H}_0$	$A\mathbb{Z}^d$	$A\mathbb{Z}_n \times \mathbb{Z} \bmod \begin{pmatrix}2\pi\\ 0\end{pmatrix}$
characters χ	$\chi_{\mathbf{k}}(\mathbf{a}) = e^{i\mathbf{k}\cdot\mathbf{a}}$	$\chi_{\alpha,\beta}(\theta, \tau) = e^{i(\alpha\theta+\beta\tau)}$
dual group H'	$\{\chi_{\mathbf{k}} : \mathbf{k} \in \mathbb{R}^d\}$	$\{\chi_{\alpha,\beta} : (\alpha, \beta) \in \mathbb{Z} \times \mathbb{R}\}$
parameter space	$\mathbb{R}^d$	$\mathbb{Z} \times \mathbb{R}$
reciprocal lattice group H_0'	$\{\chi_{\mathbf{k}} : \mathbf{k} \in 2\pi A^{-T}\mathbb{Z}^d\}$	$\{\chi_{\alpha,\beta} : \begin{pmatrix}\alpha\\ \beta\end{pmatrix} \in 2\pi A^{-T}\mathbb{Z} \times \mathbb{Z}\}$
parameter space $\mathcal{H}_0'$ (recipr. lattice)	$2\pi A^{-T}\mathbb{Z}^d$	$2\pi A^{-T}\mathbb{Z} \times \mathbb{Z}$
reciprocal lattice $\mathcal{H}_0'$ in a basis	$\{h\mathbf{b}_1 + k\mathbf{b}_2 + \ell\mathbf{b}_3 : h, k, \ell \in \mathbb{Z}\}$, $\mathbf{b}_i$ columns of $2\pi A^{-T}$ $(d = 3)$	$\{i'\begin{pmatrix}n\\ -\frac{n\theta_0}{\tau_0}\end{pmatrix} + j'\begin{pmatrix}0\\ \frac{2\pi}{\tau_0}\end{pmatrix} : i', j' \in \mathbb{Z}\}$

To derive the reciprocal lattice groups H_0' and their parameterizations $\mathcal{H}_0'$ in Table 1, we use Definition 7.1 and (5.3), (6.11). In the crystal case we obtain

$$H_0' = \{\chi_{\mathbf{k}} : \mathbf{k} \in \mathbb{R}^d, \mathbf{k}\cdot\mathbf{a} \in 2\pi\mathbb{Z} \text{ for all } \mathbf{a} \in A\,\mathbb{Z}^d\} = \{\chi_{\mathbf{k}} : \mathbf{k} \in 2\pi A^{-T}\mathbb{Z}^d\},$$

[4] In group theory, a subgroup is called a lattice subgroup if it is discrete, i.e., has no accumulation points, and there exists a set of finite volume (Haar measure) whose orbit under the subgroup gives the whole group. To derive the representation (7.2), one shows and uses that each such subgroup must be the image of a lattice subgroup of the two-dimensional translation group $\mathbb{R}^2$ under the map $h : \mathbb{R}^2 \to \mathcal{H}_{\mathbf{e}}$ defined by $h(\theta, \tau) = (\mathbf{R}_{\theta \bmod 2\pi}|\tau\mathbf{e})$, and chooses a minimal rotation as one of the generators of the group.

recovering the standard definition (3.3) of the reciprocal lattice, and in the helical case (7.3),

$$H_0' = \Big\{ \chi_{\alpha,\beta} \,:\, (\alpha,\beta) \in \mathbb{Z}\times\mathbb{R}, \quad \begin{pmatrix}\alpha\\ \beta\end{pmatrix} \cdot \begin{pmatrix}\theta\\ \tau\end{pmatrix} \in 2\pi\mathbb{Z} \text{ for all } \begin{pmatrix}\theta\\ \tau\end{pmatrix} \in A\,\mathbb{Z}_n \times \mathbb{Z} \bmod \begin{pmatrix}2\pi\\ 0\end{pmatrix} \Big\}$$
$$= \{\chi_{\alpha,\beta} \,:\, (\alpha,\beta) \in \mathcal{H}_0'\} \text{ with } \mathcal{H}_0' = 2\pi A^{-T}\mathbb{Z}\times\mathbb{Z}. \tag{7.4}$$

The parameterization $\mathcal{H}_0'$, emerging here from group theory, is precisely the reciprocal helical lattice, introduced in [KCW58] in the context of fiber diffraction via physical considerations. See Figure 4.

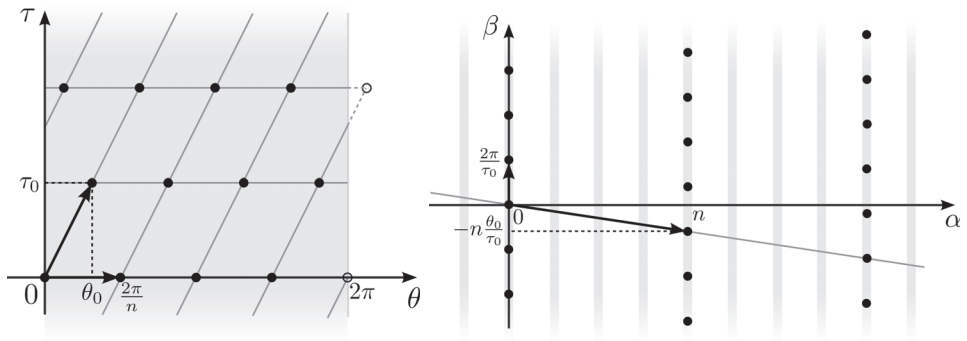

FIG. 4. *A discrete helical group (left,* (7.3)*) and the associated reciprocal helical lattice (right,* (7.4)*). Here θ is the rotation angle about the helical axis and τ the displacement along the axis, and the reciprocal parameters α and β are the angular and the axial wavenumber. The slope of the reciprocal basis vector pointing to the right is the inverse pitch multiplied by 2π. The discrete helical group is a subset of the continuous helical group $\mathcal{H}_{\mathbf{e}} \doteq S^1 \times \mathbb{R}$ (*(6.1)*, shaded vertical strip), whereas the reciprocal helical lattice is a subset of the dual group $\mathbb{Z}\times\mathbb{R}$ (shaded vertical lines).*

8. Diffraction of twisted waves: Twisted Von Laue condition. We now calculate the outgoing radiation when twisted waves are scattered off helical structures of infinite length. The existence and location of resonant parameter values can be derived in an elementary manner [JFJ16]. The complete analysis here recovers this result via a Poisson summation formula on the helical group, and in addition establishes the vanishing of the signal elsewhere, i.e., a sharp peak structure, and the peak strengths.

The key point is to evaluate the structure factor (2.12) when $\mathbf{E}_0$ is a twisted wave (6.4) with parameters $(\alpha,\beta,\gamma) \in \mathbb{Z}\times\mathbb{R}\times(0,\infty)$.

In the case of an axial detector, we will proceed in three steps: (1) transform to cylindrical coordinates; (2) treat the integration over $\varphi' \in S^1$ and $z' \in \mathbb{R}$ jointly rather than separately, because these variables are "intertwined" in the electron density of a helical structure, and use Fourier calculus on the group $S^1\times\mathbb{R}$ to essentially reduce the integral to the Fourier transform of an infinite sum of delta functions on $S^1\times\mathbb{R}$; (3) apply the Poisson summation formula. In the case of a nonaxial detector, treated in the supplementary material (M104341_01.pdf [local/web 246KB]), two additional steps are necessary: (1b) eliminate the ensuing phase nonlinearity of the plane-wave factor inside the integral (2.12) by expanding this plane wave into cylindrical waves,

which mathematically corresponds to a Fourier series expansion in the angle variable; (3b) eliminate the expansion of step 1b in the case of a nonaxial detector.

Step 1 (cylindrical coordinates). Let (r,φ,z) and (r',φ',z') be cylindrical coordinates for $\mathbf{x}$ and $\mathbf{y}$; i.e., $\mathbf{x}$ is given by (6.2) and $y_1 = r'\cos\varphi'$, $y_2 = r'\sin\varphi'$, $y_3 = z'$. Next, let (R,Φ,Z) be the cylindrical components of the outgoing wavevector field $\mathbf{k}'(r,\varphi,z)$, i.e., $\mathbf{k}' = R\mathbf{e}_r + \Phi\mathbf{e}_\varphi + Z\mathbf{e}_z$, where $\mathbf{e}_r$, $\mathbf{e}_\varphi$, and $\mathbf{e}_z$ are the usual cylindrical unit vectors. It follows that

$$R(r,\varphi,z) = \frac{\omega}{c}\frac{r}{\sqrt{r^2+z^2}},\quad \Phi(r,\varphi,z) = 0,\quad Z(r,\varphi,z) = \frac{\omega}{c}\frac{z}{\sqrt{r^2+z^2}}. \tag{8.1}$$

In the special case of an axial detector, i.e., $(r,\varphi,z) = (0,0,z)$, the cylindrical components of the outgoing wavevector $\mathbf{k}'(r,\varphi,z)$ are

$$R = 0,\quad \Phi = 0,\quad Z = \frac{\omega}{c}\operatorname{sign}(z). \tag{8.2}$$

Thus it follows from (2.6), (2.12) that

$$\begin{aligned}\mathbf{f}_{\mathbf{E}_0}(\mathbf{k}'(0,0,z)) = \mathbf{N}(\mathbf{n})\int_0^\infty \Bigg[\int_{S^1\times\mathbb{R}} \rho(r',\varphi',z') \\ \cdot \begin{pmatrix} e^{i[(\alpha+1)\varphi'+(\beta-Z)z']} & & \\ & e^{i[(\alpha-1)\varphi'+(\beta-Z)z']} & \\ & & e^{i[\alpha\varphi'+(\beta-Z)z']}\end{pmatrix} d\varphi' dz'\Bigg] \begin{pmatrix} J_{\alpha+1}(\gamma r') \\ J_{\alpha-1}(\gamma r') \\ J_\alpha(\gamma r')\end{pmatrix} r' dr'.\end{aligned} \tag{8.3}$$

Step 2 (exploit helical symmetry and Fourier calculus on $S^1\times\mathbb{R}$). Consider now a helical structure, i.e., a structure generated by any discrete helical group H_0 (see (7.3)). The electron density ρ will be H_0-periodic, that is, in cylindrical coordinates,

$$\rho(r',\varphi',z') = \rho(r',\varphi'-\theta \bmod 2\pi, z'-\tau) \text{ for all } \begin{pmatrix}\theta\\ \tau\end{pmatrix} \in \mathcal{H}_0,\ \mathcal{H}_0 = A\,\mathbb{Z}_n\times\mathbb{Z} \bmod \begin{pmatrix}2\pi\\ 0\end{pmatrix},$$

and rapidly decaying in the direction perpendicular to the helical axis. Typical examples of H_0-periodic densities are depicted in Figure 5. By choosing a suitable partition of unity, such a ρ can be written as a sum of rotated and translated copies of a localized, rapidly decaying function ψ,

$$\rho(r',\varphi',z') = \sum_{\mathbf{a}\in\mathcal{H}_0} \psi(r',\varphi'-a_1 \bmod 2\pi, z'-a_2). \tag{8.4}$$

The function ψ can, for instance, be taken as the restriction of ρ to the unit cell $\mathcal{U}$ of the structure,

$$\psi = \rho_{\mathcal{U}} = \begin{cases}\rho & \text{in } \mathcal{U},\\ 0 & \text{outside } \mathcal{U},\end{cases} \qquad \mathcal{U} = \{(r',\varphi',z') \,:\, (\varphi',z') \in A\,[0,1]^2,\ r'\in(0,\infty)\}, \tag{8.5}$$

but other constructions with a smooth ψ make sense too.

The decomposition (8.4) of ρ can be fruitfully rewritten as a convolution of ψ with an infinite sum of delta functions,

$$\rho = \psi *_{S^1\times\mathbb{R}} \delta_{\mathcal{H}_0},\quad \delta_{\mathcal{H}_0} = \sum_{\mathbf{a}\in\mathcal{H}_0}\delta_{\mathbf{a}},$$

where the convolution on $S^1 \times \mathbb{R}$ is defined as

$$(f *_{S^1\times\mathbb{R}} g)(r,\varphi,z) = \int_{S^1\times\mathbb{R}} f(r,\varphi-\varphi' \bmod 2\pi, z-z')\, g(r,\varphi',z')\, d\varphi' dz'. \tag{8.6}$$

In what follows we drop the subscript from the convolution sign. We now use Fourier calculus on $S^1 \times \mathbb{R}$. The Fourier transform $\mathcal{F}_{S^1\times\mathbb{R}}$ with respect to the angle and axis variables is a function on the dual group $(S^1 \times \mathbb{R})' \cong \mathbb{Z} \times \mathbb{R}$, defined as

$$(\mathcal{F}_{S^1\times\mathbb{R}} f)(r,\Phi,Z) = \frac{1}{2\pi}\int_{S^1\times\mathbb{R}} f(r,\varphi,z)\, e^{-i(\Phi\,\varphi + Z\,z)} d\varphi\, dz. \tag{8.7}$$

The square bracket in (8.3) has the form of such a Fourier transform on $S^1 \times \mathbb{R}$; for instance, the top left component of the square bracket equals $2\pi(\mathcal{F}_{S^1\times\mathbb{R}}(\psi * \delta_{\mathcal{H}_0})(r', -(\alpha+1), Z-\beta)$.

Step 3 (Poisson summation formula on $S^1 \times \mathbb{R}$). We now use the (trivial) convolution rule on $S^1 \times \mathbb{R}$,

$$\mathcal{F}_{S^1\times\mathbb{R}}(f * g) = 2\pi\, \mathcal{F}_{S^1\times\mathbb{R}} f \cdot \mathcal{F}_{S^1\times\mathbb{R}} g, \tag{8.8}$$

and the following nontrivial result from Fourier analysis on abelian groups which makes the reciprocal helical lattice appear:

LEMMA 8.1 (Poisson summation formula on $S^1 \times \mathbb{R}$). *Let H_0 be any discrete helical group (see* (7.3)*), and let H_0' be the reciprocal lattice group. The corresponding parameterizations $\mathcal{H}_0 \subset S^1 \times \mathbb{R}$, see* (7.3)*, and $\mathcal{H}_0' \subset \mathbb{Z} \times \mathbb{R}$, see* (7.4)*, satisfy*

$$\mathcal{F}_{S^1\times\mathbb{R}} \delta_{\mathcal{H}_0} = \frac{2\pi}{|\det A|}\, \delta_{\mathcal{H}_0'}. \tag{8.9}$$

This identity is a special case of the general Poisson formula on locally compact abelian groups going back to Weil [We64]; see, e.g., [RS00].[5] A more elementary derivation of (8.9) is to first consider the case $\theta = 0$, where the result follows by combining the usual Poisson formula on $\mathbb{R}$,

$$\widehat{\delta_{a\mathbb{Z}}} = \tfrac{2\pi}{a}\delta_{\frac{2\pi}{a}\mathbb{Z}},$$

with the following, elementary to check, Poisson formula on S^1: if $\mathcal{L} = \{\frac{2\pi j}{n} : j = 0,\dots,n-1\}$, then

$$\delta_{\mathcal{L}}(\varphi) = \sum_{j=0}^{n-1} \delta_{\frac{2\pi j}{n}}(\varphi),\ \varphi \in [0,2\pi), \qquad \widehat{\delta_{\mathcal{L}}}(\nu) = \frac{n}{2\pi}\delta_{n\mathbb{Z}}(\nu) = \frac{n}{2\pi}\sum_{a\in n\mathbb{Z}} \delta_a(\nu),\ \nu \in \mathbb{Z}.$$

Here $\hat{f}(\nu)$ denotes the Fourier coefficient $(2\pi)^{-1}\int_0^{2\pi} e^{-i\nu\varphi} f(\varphi)\, d\varphi$. Note that the delta functions in the left sum are Dirac deltas, whereas the delta functions in the right sum are Kronecker deltas. The general result (8.9) now follows from a suitable change of variables.

Equations (8.8), (8.9) yield

$$\mathcal{F}_{S^1\times\mathbb{R}}(\psi * \delta_{\mathcal{H}_0}) = \frac{(2\pi)^2}{|\det A|}(\mathcal{F}_{S^1\times\mathbb{R}}\psi)\cdot \delta_{\mathcal{H}_0'}, \tag{8.10}$$

[5] In this context, the formula is stated and derived up to an overall multiplicative constant.

and therefore

(8.11)

$$\mathbf{f}_{\mathbf{E}_0}(\mathbf{k}'(0,0,z)) = \frac{(2\pi)^3}{|\det A|}\,\mathbf{N}(\mathbf{n}) D_{\alpha,\beta,\gamma}(R,Z) \begin{pmatrix} \delta_{\mathcal{H}_0'}(-(\alpha+1), Z-\beta) \\ \delta_{\mathcal{H}_0'}(-(\alpha+1), Z-\beta) \\ \delta_{\mathcal{H}_0'}(-\alpha, Z-\beta) \end{pmatrix},$$

$$\text{with } D_{\alpha,\beta,\gamma}(R,Z) = \int_0^\infty \begin{pmatrix} \mathcal{F}_{S^1\times\mathbb{R}}\psi(-(\alpha+1), Z-\beta) J_{\alpha+1}(\gamma r') & 0 & 0 \\ 0 & \mathcal{F}_{S^1\times\mathbb{R}}\psi(-(\alpha-1), Z-\beta) J_{\alpha-1}(\gamma r') & 0 \\ 0 & 0 & \mathcal{F}_{S^1\times\mathbb{R}}\psi(-\alpha, Z-\beta) J_\alpha(\gamma r') \end{pmatrix} r' dr'.$$

The matrix components of the above integral can be interpreted as a *Hankel transform*. Recall that for any $\alpha \in \mathbb{Z}$, the Hankel transform of order α maps scalar functions of a radial variable belonging to the interval $(0,\infty)$ to scalar functions on $(0,\infty)$ and is defined as

$$(H_\alpha f)(\gamma) = \int_0^\infty f(r')\, J_\alpha(\gamma r')\, r' dr' \quad (\gamma > 0). \tag{8.12}$$

This together with the fact that $\delta_{\mathcal{H}_0'} = \sum_{\mathbf{a}\in\mathcal{H}_0'} \delta_{\mathbf{a}'}$ and $\delta_{\mathbf{a}'}(-(\alpha \pm 1), Z-\beta) = \delta_{\mathbf{a}'\pm(1,0)}(-\alpha, Z-\beta)$ yields

(8.13)

$$\mathbf{f}_{\mathbf{E}_0}(\mathbf{k}'(0,0,z)) = \frac{(2\pi)^3}{|\det A|}\,\mathbf{N}(\mathbf{n}) \sum_{\mathbf{a}'\in\mathcal{H}_0'} \left(H_{-a_1'} \mathcal{F}_{S^1\times\mathbb{R}}\psi\right)(\gamma, \mathbf{a}') \begin{pmatrix} \delta_{\mathbf{a}'+\binom{1}{0}} \\ \delta_{\mathbf{a}'-\binom{1}{0}} \\ \delta_{\mathbf{a}'} \end{pmatrix} (-\alpha, Z-\beta).$$

Note that the delta functions in (8.13) are centered on shifted copies of the reciprocal lattice. Also, we claim that the Fourier–Hankel transform of ψ which appears in (8.13) equals that of the electron density (8.5) in the unit cell, i.e., $H_{-a_1'}\mathcal{F}_{S^1\times\mathbb{R}}\psi(\gamma,\mathbf{a}') = H_{-a_1'}\mathcal{F}_{S^1\times\mathbb{R}}\rho_{\mathcal{U}}(\gamma,\mathbf{a}')$ for all $\mathbf{a}' \in \mathcal{H}_0'$. This is because, for any ψ satisfying (8.4), including $\psi = \rho_U$, the Fourier transform $(\mathcal{F}_{S^1\times\mathbb{R}}\psi)(r',\mathbf{a}')$ is independent of ψ when $\mathbf{a}'$ is a reciprocal lattice vector; indeed,

$$\begin{aligned}(\mathcal{F}_{S^1\times\mathbb{R}}\psi)(R',\mathbf{a}') &= \int_{S^1\times\mathbb{R}} e^{i\mathbf{a}'\cdot\binom{\varphi'}{z'}} \psi(r',\varphi',z') d\varphi' dz' \\ &= \sum_{\mathbf{a}\in\mathcal{L}} \int_{\mathcal{U}} e^{-i\mathbf{a}'\cdot\left(\binom{\varphi'}{z'}-\mathbf{a}\right)} \psi(r', \varphi' - a_1 \bmod 2\pi, z'-a_2)\, d\varphi' dz',\end{aligned}$$

and the factors $e^{i\mathbf{a}'\cdot\mathbf{a}}$ above equal 1, allowing one to eliminate ψ via (8.4).

The outgoing electric field can now be read off immediately from (2.5), (2.6), (2.12), (8.13), and the fact that we may take $\psi = \rho_U$. Note in particular that the third field component vanishes, since the projection matrix in (2.5) annihilates the third component of the structure factor when the outgoing wavevector $\mathbf{k}'$ points in axial direction $\pm\mathbf{e}_3$. See (8.14) below.

When taking absolute values to obtain the intensity, it may happen that the two remaining shifted copies $\mathcal{H}_0' + (1,0)$ and $\mathcal{H}_0' - (1,0)$ of the reciprocal lattice appearing in (8.13) overlap, which would lead to interference. These two copies overlap if and only if $(2,0)$ is a reciprocal helical lattice vector. The following result, which is elementary to check, shows that this does not happen except in a degenerate case which we propose to denote *flat helical groups*.

LEMMA 8.2 (flat helical groups). *The following three statements about a discrete helical group* (7.2) *are equivalent:*

(1) *The vector* $(2,0)$ *belongs to the reciprocal helical lattice,* (7.4).
(2) *The parameters of the helical group satisfy* $\theta_0 = 0$ *or* π, *and* $n = 1$ *or* 2.
(3) *The structure generated by applying the helical group to any single point lies in a plane.*

We summarize our findings as a theorem.

THEOREM 8.3 (twisted Von Laue condition). *Consider an infinitely long helical structure with electron density* $\rho : \mathbb{R}^3 \to \mathbb{R}$, *assumed to be smooth,* H_0*-periodic with respect to some discrete helical group* H_0 *(see* (7.2)*), and rapidly decaying in the direction perpendicular to the helical axis. Assume that the axis is* $\mathbf{e} = \mathbf{e}_3$, *and let the incoming electric field be a twisted wave with same axis and parameter vector* $(\alpha, \beta, \gamma) \in \mathbb{Z} \times \mathbb{R} \times (0, \infty)$ *(see* (6.4)–(6.6)*). Then the diffracted electric field* (2.5) *at any point* $(0,0,z)$ *on the axis is*

$$\mathbf{E}_{out}(0,0,z,t) = -c_{e\ell}\frac{e^{i(\frac{\omega}{c}|z|-\omega t)}}{|z|}\frac{(2\pi)^3}{|\det A|}\sum_{\mathbf{a}'\in\mathcal{H}_0'}(H_{-a_1'}\mathcal{F}_{S^1\times\mathbb{R}}\rho_{\mathcal{U}})(\gamma,\mathbf{a}') \cdot \begin{pmatrix} \frac{n_1+in_2}{2} & \frac{n_1-in_2}{2} & 0 \\ \frac{n_2-in_1}{2} & \frac{n_2+in_1}{2} & 0 \\ 0 & 0 & 0 \end{pmatrix} \begin{pmatrix} \delta_{\mathbf{a}'+\binom{1}{0}} \\ \delta_{\mathbf{a}'-\binom{1}{0}} \\ 0 \end{pmatrix} (-\alpha, \tfrac{\omega}{c}\operatorname{sign} z - \beta). \tag{8.14}$$

Here H_α *is the Hankel transform of order* α *with respect to the radial variable (see* (8.12)*),* $\mathcal{F}_{S^1\times\mathbb{R}}$ *is the Fourier series/transform with respect to the angular and axial variables (see* (8.7)*),* $\rho_{\mathcal{U}}$ *is the restriction of the electron density* ρ *to the unit cell (see* (8.5)*), and* $\mathcal{H}_0'$ *is the reciprocal helical lattice (see* (7.4)*).*

Moreover, when H_0 *is not a flat helical group (see Lemma* 8.2*), the square root of the outgoing intensity is*

$$\Big(I(0,0,z;\,\alpha,\beta,\gamma)\Big)^{1/2} = c_0\frac{(2\pi)^3}{|\det A|}\frac{1}{|z|}\sum_{\mathbf{a}'\in\mathcal{H}_0'}\Big|(H_{-a_1'}\mathcal{F}_{S^1\times\mathbb{R}}\rho_{\mathcal{U}})(\gamma,\mathbf{a}')\Big| \cdot \left(\frac{|n_1+in_2|}{\sqrt{2}}\delta_{\mathbf{a}'+\binom{1}{0}} + \frac{|n_1-in_2|}{\sqrt{2}}\delta_{\mathbf{a}'-\binom{1}{0}}\right)(-\alpha,\, \tfrac{\omega}{c}\operatorname{sign} z - \beta), \tag{8.15}$$

where $c_0 = (\frac{c\varepsilon_0}{2})^{1/2}c_{e\ell}$. *In particular, constructive interference occurs if and only if the difference between the angular/axial part* $(0, \frac{\omega}{c}\operatorname{sign} z)$ *of the outgoing wavevector and the angular/axial parameters* (α,β) *of the incoming twisted wave belongs to the reciprocal helical lattice shifted left or right by precisely one angular wavenumber,* $\mathcal{H}_0' \pm \binom{1}{0}$, *or equivalently, if and only if*

$$\begin{pmatrix} \alpha+\sigma \\ \beta - 2\pi/\lambda \end{pmatrix} = i'\begin{pmatrix} n \\ -n\theta_0/\tau_0 \end{pmatrix} + j'\begin{pmatrix} 0 \\ 2\pi/\tau_0 \end{pmatrix} \quad \textit{for some integers } i',\, j' \textit{ and } \sigma = \pm 1. \tag{8.16}$$

Formulae (8.14), (8.15), (8.16) are the main result of this paper and were announced in [JFJ16]. They say that the signal of a helical structure under co-axial twisted X-rays, recorded along the axis, consists of sharp peaks with respect to the angular and axial radiation parameters. The peaks are *double-peaks* with a distance

of precisely two angular wavenumbers, centered at the reciprocal lattice vectors of the helical structure. In particular, at the reciprocal lattice vectors themselves the signal vanishes. The structural parameters τ_0, θ_0 in (7.2), or equivalently the pitch and the number of subunits per turn, can be immediately read off from the peak locations, as can the order n of any rotational symmetry.

Moreover, the above result makes it in principle possible to determine the electron density ρ, i.e., the detailed atomic structure, from intensity measurements in the far field at a specific point on the axis, provided the scalar phase problem associated with the Fourier–Hankel transform $H_\alpha \mathcal{F}_{S^1\times\mathbb{R}}$ can be solved. Note that the values of this transform on the reciprocal helical lattice points which appear in (8.15) completely determine the electron density; see section 9 for details.

Next, we report an important invariance property of the axial signal of a helical structure. Suppose the structure is translated by an amount Δz along the helical axis and rotated by an amount $\Delta\varphi$ around the axis. (In other words, we apply an arbitrary element of the continuous helical group (6.1) to the structure.) This modifies the original electron density $\rho_{\mathcal{U}}$ to

$$\rho_{\mathcal{U}}{}'(r,\varphi,z) = \rho_{\mathcal{U}}(r,\varphi-\Delta\varphi,z-\Delta z). \tag{8.17}$$

From the definition of the angular/axial Fourier transform, (8.7), and the Hankel transform, (8.12), it is clear that

$$\Big(H_{-\alpha}\mathcal{F}_{S^1\times\mathbb{R}}\rho'_{\mathcal{U}}\Big)(\gamma,\Phi,Z) = e^{-i(\Phi\,\Delta\varphi+Z\,\Delta z)}\Big(H_{-\alpha}\mathcal{F}_{S^1\times\mathbb{R}}\rho_{\mathcal{U}}\Big)(\gamma,\Phi,Z) \quad \text{for all } \gamma,\ \Phi,\ Z. \tag{8.18}$$

Thus the outgoing intensity (8.15), which only depends on the absolute value of the expression (8.18), is *invariant* under axial translations and rotations of the structure. This is not a fortuitous accident, but stems from the fact that the design equations, (4.9), require the incoming wave to be an eigenfunction of each element of the continuous helical group (6.1). From this one easily sees that the invariance remains true for helical structures of finite length.

By comparison, the signal produced by fiber diffraction, i.e., by sending plane wave X-rays towards a helical structure from a perpendicular direction, is only invariant under axial translation but *not* under axial rotation; the latter is a well-known major problem in the interpretation of fiber diffraction images.

9. Synthesis of electron density. As shown in the previous section, subjecting a helical structure to twisted X-rays and recording the intensity of the scattered radiation in axial direction yields the data set

$$\left\{|G(\gamma,\alpha,\beta)|^2 \,:\, \gamma\in(0,\infty),\ (\alpha,\beta)\in\mathcal{H}_0'\right\}, \tag{9.1}$$

where G is the Fourier–Hankel transform of the unit cell electron density $\rho_{\mathcal{U}}$,

$$\begin{aligned} G(\gamma,\alpha,\beta) &= \Big(H_{-\alpha}\mathcal{F}_{S^1\times\mathbb{R}}\rho_{\mathcal{U}}\Big)(\gamma,\alpha,\beta)\\ &= \frac{1}{2\pi}\int_0^\infty\iint_{\mathcal{U}} e^{-i(\alpha\varphi+\beta z)}J_{-\alpha}(\gamma r)\,\rho_{\mathcal{U}}(r,\varphi,z)\,r\,dr\,d\varphi\,dz, \end{aligned} \tag{9.2}$$

and $\mathcal{H}_0'$ is the reciprocal helical lattice of the structure. Assume that the phases of the Fourier–Hankel coefficients G in (9.1) can be retrieved. Then the electron density in the unit cell is recovered by

$$\rho_{\mathcal{U}}(r,\varphi,z) = \frac{1}{2\pi} \sum_{\binom{\alpha}{\beta}\in\mathcal{H}_0'} (-1)^\alpha \int_0^\infty J_\alpha(\gamma r)\, G(\gamma,\alpha,\beta)\, \gamma\, d\gamma\, e^{i(\alpha\varphi+\beta z)}. \tag{9.3}$$

When indexing the reciprocal helical lattice points in $\mathcal{H}_0'$ by pairs of integers (i',j') according to the representation $(\alpha,\beta) = i'\mathbf{b}_1 + j'\mathbf{b}_2$, where $\mathbf{b}_1 = (n, -n\theta_0/\tau_0)$, $\mathbf{b}_2 = (0, 2\pi/\tau_0)$ are the basis vectors of the reciprocal helical lattice (7.4), and denoting $\frac{1}{2\pi}(-1)^\alpha G(\gamma,\alpha,\beta) = G_{i'j'}(\gamma)$, equation (9.3) acquires the form announced in [JFJ16],

$$\rho_{\mathcal{U}}(r,\varphi,z) = \sum_{i',j'} \int_0^\infty \gamma\, d\gamma\, G_{i'j'}(\gamma)\, J_{i'n}(\gamma r) e^{i(i'\mathbf{b}_1+j'\mathbf{b}_2)\cdot\binom{\varphi}{z}}. \tag{9.4}$$

To establish (9.3), one first notes that the Fourier–Hankel transform in (9.2) is a combination of a Fourier series in the angle, a Fourier transform in the axial variable, and a Hankel transform in the radial variable, and it is thus invertible. One then exploits formula (8.10) with $\psi = \rho_U$, and uses that $J_{-\alpha} = (-1)^\alpha J_\alpha$ and that the inverse of the Hankel transform (8.12) is given by $(H_\alpha^{-1}\tilde{f})(r) = \int_0^\infty \tilde{f}(\gamma)\, J_\alpha(\gamma r)\, \gamma\, d\gamma$. The overall situation is thus the same as in standard X-ray crystallography: the electron density can be reconstructed provided we can solve a scalar phase problem. The only difference is that we have to deal with the following new phase problem:

NEW PHASE PROBLEM. *Reconstruct a function ρ_U given the absolute value of its Fourier–Hankel transform G defined by* (9.2).

Numerical investigations which are reported elsewhere [JFJ16] indicate that standard phase retrieval algorithms for the Fourier transform can be adapted without difficulty to the Fourier–Hankel case.

10. Simulated diffraction pattern of carbon nanotube and tobacco mosaic virus. Here we present simulated diffraction patterns of helical structures subjected to twisted waves. The set-up is as in Figure 2 of the introduction; that is, incoming waves, structure, and detector are axially aligned.

We consider two examples, a (6,5)-Carbon nanotube and TMV virus. The parameters are as in Example 1 (respectively, Example 2) of section 7, with the TMV atomic positions taken from the Protein Data Bank, PDB ID 3J06 [GZ11]. We use the electromagnetic model (2.5), (2.6), (2.10) to calculate the signal from structures of finite length:

- *C nanotube*: 255 unit cells, corresponding to 510 atoms.
- *TMV*: 147 proteins, corresponding to three helical repeats and 188 748 atoms.

The results in Figure 5 show that already relatively short pieces of a helical structure exhibit the theoretically predicted patterns. In particular, one sees double-peaks centered at the reciprocal helical lattice points which would be difficult to interpret correctly in terms of scalar models of the incoming wave and the diffraction pattern. Moreover, very high contrast between peaks and background is observed; note that in fiber diffraction the contrast in the direction perpendicular to the fiber is limited for theoretical reasons [CCV52].

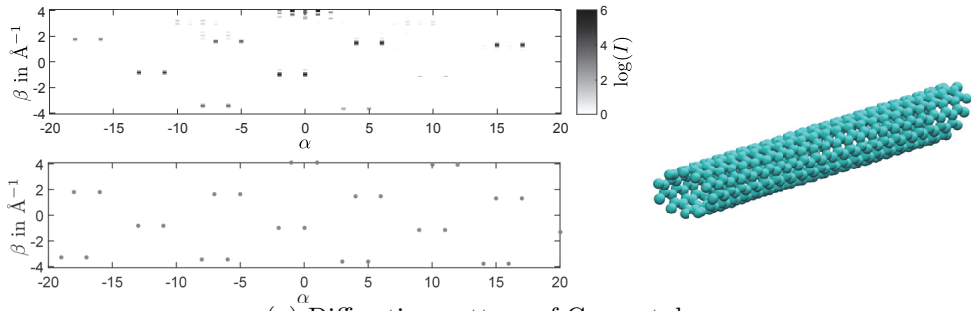

(a) Diffraction pattern of C nanotube

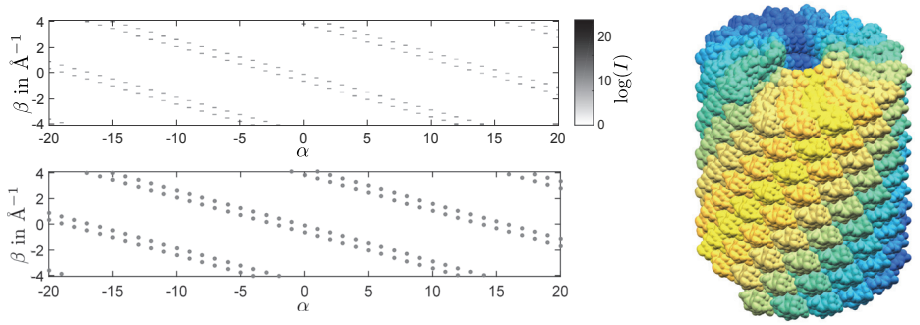

(b) Diffraction pattern of TMV virus

FIG. 5. *Twisted X-ray pattern of* (a) *a* (6,5)*-carbon nanotube with* 510 *atoms,* (b) *three helical repeats of TMV (*147 *proteins,* 188 748 *atoms). The electron density of each atom was modeled by a Gaussian.* (a) *and* (b)*, right: Isosurface of electron density.* (a) *and* (b)*, top: Log intensity of diffracted radiation as a function of angular wavenumber* α *and axial wavenumber* β *of the incoming wave. In* (b)*, for simplicity atomic form factors were ignored and the electron density of each atom was approximated by a delta function.* (a) *and* (b)*, bottom: Theoretical peak locations,* (8.15), (8.16)*. Incoming twisted X-ray wavelength:* $\lambda = 1.54$ A^o *(Cu* K_α *line).*

11. Conclusions and outlook. We have shown on the level of modeling and simulation that twisted X-ray waves would be a very promising tool for structure analysis.

Numerous theoretical challenges remain. For helical structures, a better understanding of the outgoing radiation in nonaxial direction would be desirable. A related issue is to develop a general mathematical theory of the "radiation transform," (2.12), which takes the role of the Fourier transform when the incoming radiation is not given by plane waves. Robust phase retrieval algorithms need to be developed for structure reconstruction from twisted X-ray data. And for structures generated by non-abelian symmetry groups such as buckyballs, the right incoming waveforms are not clear; for reasons discussed at the end of section 4, in this case the design equations may not be the right approach.

Challenges for the experimental realization include: generation of tunable coherent twisted X-ray waves with a broad spectrum of angular wavenumbers; axial alignment of incoming wave and structure; and achieving a sufficiently strong outgoing signal.

Acknowledgments. GF and RDJ thank Dominik Schryvers for helpful discussions on vortex beams. GF thanks John Ockendon for helpful discussions which led to the spectral interpretation of twisted waves and Robin Santra for providing advice

and reference [Sa09] on the derivation of X-ray diffraction intensities from quantum electrodynamics.

REFERENCES

[AB92] L. Allen, M. W. Beijersbergen, R. J. C. Spreeuw, and J. P. Woerdman, *Orbital angular momentum of light and the transformation of Laguerre-Gaussian laser modes*, Phys. Rev. Lett., 45 (1992), pp. 8185–8189.

[AD00] J. Arlt and K. Dholakia, *Generation of high-order Bessel beams by use of an axicon*, Opt. Commun., 177 (2000), pp. 297–301.

[AM11] J. Als-Nielsen and D. McMorrow, *Elements of Modern X-Ray Physics*, John Wiley and Sons, New York, 2011.

[AM76] N. W. Ashcroft and N. D. Mermin, *Solid State Physics*, Saunders College Publishing, Philadelphia, 1976.

[BG08] M. Baake and U. Grimm, *The singular continuous diffraction measure of the Thue–Morse chain*, J. Phys. A, 41 (2008), 422001.

[BG13] M. Baake and U. Grimm, *Aperiodic Order: Volume* 1: *A Mathematical Invitation*, Cambridge University Press, Cambridge, UK, 2013.

[BM04] M. Baake and R. Moody, *Weighted Dirac combs with pure point diffraction*, J. Reine Angew. Math., 573 (2004), pp. 61–94.

[CCV52] W. Cochran, F. H. C. Crick, and V. Vand, *The structure of synthetic polypeptides.* I. *The transform of atoms on a helix*, Acta Cryst., 5 (1952), pp. 581–586.

[CK62] D. L. D. Caspar and A. Klug, *Physical principles in the construction of regular viruses*, Cold Spring Harbor Symp. Quant. Biol., 27 (1962), pp. 1–24.

[CT97] C. Cohen-Tannoudji, J. Dupont-Roc, and G. Grynberg, *Photons and Atoms: Introduction to Quantum Electrodynamics*, Wiley, New York, 1997.

[DEJ] K. Dayal, R. Elliott, and R. D. James, *Objective Formulas*, unpublished manuscript.

[Di75] J. Dieudonné, *Éléments d'analyse*, Vol. 6, Gauthier-Villars, Paris, 1975.

[FJJ16] G. Friesecke, R. D. James, and D. Jüstel, *Mathematical Models of X-Ray Diffraction Patterns*, manuscript.

[FKL12] W. Friedrich, P. Knipping, and M. von Laue, *Interferenzerscheinungen bei Röntgenstrahlen*, Sitzungsberichte der Mathematisch-Physikalischen Classe der Königlich-Bayerischen Akademie der Wissenschaften zu München, 1912.

[Fr07] G. Friesecke, *Lectures on Fourier Analysis*, lecture notes, University of Warwick, Coventry, UK, 2007.

[Gr99] D. J. Griffiths, *Introduction to Electrodynamics*, Prentice–Hall, Upper Saddle River, NJ, 1999.

[GZ11] P. Ge and Z. H. Zhou, *Hydrogen-bonding networks and RNA bases revealed by cryo electron microscopy suggest a triggering mechanism for calcium switches*, Proc. Natl. Acad. Sci. USA, 108 (2011), pp. 9637–9642.

[Ha34] W. W. Hansen, *Transformations useful in certain antenna calculations*, J. Appl. Phys., 8 (1937), pp. 282–286.

[HD92] N. R. Heckenberg, R. McDuff, C. P. Smith, and A. G. White, *Generation of optical phase singularities by computer generated holograms*, Opt. Lett., 17 (1992), pp. 221–223.

[Ho95] A. Hof, *On diffraction by aperiodic structures*, Comm. Math. Phys., 169 (1995), pp. 25–43.

[HR63] E. Hewitt and K. A. Ross, *Abstract Harmonic Analysis* I, Springer, Berlin, 1963.

[Ja06] R. D. James, *Objective structures*, J. Mech. Phys. Solids, 54 (2006), pp. 2354–2390.

[Ja98] J. D. Jackson, *Classical Electrodynamics*, John Wiley and Sons, New York, 1998.

[JFJ16] D. Jüstel, G. Friesecke, and R. D. James, *Bragg-Von Laue diffraction generalized to twisted X-rays*, Acta Cryst., A72 (2016), pp. 190–196.

[Ju16] D. Jüstel, *The Zak Transform on Strongly Proper G-Spaces and Its Applications*, preprint, arXiv:1605.05168, 2016.

[KCW58] A. Klug, F. H. C. Crick, and H. W. Wyckoff, *Diffraction by helical structures*, Acta Cryst., 11 (1958), pp. 199–213.

[La15] R. Lasser, *Harmonic Analysis on Hypergroups*, World Scientific, in preparation.

[MTT07] G. Molina-Terriza, J. P. Torres, and L. Torner, *Twisted photons*, Nat. Phys., 3 (2007), pp. 305–310.

[RS00] H. Reiter and J. D. Stegeman, *Classical Harmonic Analysis and Locally Compact Groups*, Oxford University Press, New York, 2000.

[Sa09] R. Santra, *Concepts in X-ray physics*, J. Phys. B: At. Mol. Opt. Phys., 42 (2009), 023001.

[St94] R. Strichartz, *A Guide to Distribution Theory and Fourier Transforms*, CRC Press, Boca Raton, FL, 1994.

[UT10] M. Uchida and A. Tonomura, *Generation of electron beams carrying orbital angular momentum*, Nature, 464 (2010), pp. 737–739.

[VTS10] J. Verbeeck, H. Tian, and P. Schattschneider, *Production and application of electron vortex beams*, Nature, 467 (2010), pp. 301–304.

[We64] A. Weil, *Sur certains groupes d'opérateurs unitaires*, Acta Math., 111 (1964), pp. 143–211.

[Wi31] E. Wigner, *Gruppentheorie und ihre Anwendung auf die Quantenmechanik der Atomspektren*, Vieweg, Braunschweig, 1931.